

## REVIEW

[View Article Online](#)  
[View Journal](#) | [View Issue](#)Cite this: *Mater. Adv.*, 2022,  
3, 6707Received 16th June 2022,  
Accepted 24th July 2022

DOI: 10.1039/d2ma00695b

[rsc.li/materials-advances](https://rsc.li/materials-advances)

# Current challenges and future applications of antibacterial nanomaterials and chitosan hydrogel in burn wound healing

Que Bai, Caiyun Zheng, Wenting Chen, Na Sun, Qian Gao, Jinxi Liu, Fangfang Hu, SaHu Pimpi, Xintao Yan, Yanni Zhang\* and Tingli Lu \*

Burns are one of the most devastating skin injuries, with severe burns affecting almost every organ system, and that causes a high mortality rate. The presence of microbial infection in burn wounds makes the healing process more complex, leading to delayed wound healing. Therefore, the primary problem in treating burns is to developing antimicrobial biomaterials to overcome bacterial infection. The present review covers burn classification, the burn wound healing process, and various local treatment methods to fight infection and promote healing. We discussed the recent progress in the treatment of burn wound infection. We provided information on the application of antimicrobial materials in burn treatment in recent years, especially nanoparticles and chitosan hydrogels. We also discuss the promising future therapies for burns and the prospects and limitations for eventual translation to the clinic.

## 1. Introduction

Burns are the fourth most common type of trauma worldwide, coming after traffic injuries, falls, and interpersonal violence.<sup>1,2</sup>

According to the latest report from the World Health Organization, an estimated 265 000 people die every year due to burn injuries.<sup>3</sup> Burns can be caused by friction, heat, radiation, chemistry, or electric sources, but most burn injuries are caused by heat from hot liquids, solids or fire. Although all burn injuries involve tissue damage due to energy transfer, different causes may lead to different physiological and pathological damage.<sup>4,5</sup> For example, a flame can immediately cause a deep burn, whereas hot liquids or steam tend to appear more superficial initially due to rapid dilution of the source and

Key Laboratory of Space Bioscience and Biotechnology, School of Life Sciences,  
Northwestern Polytechnical University, Xi'an 710072, China.

E-mail: [yann.zhang@nwpu.edu.cn](mailto:yann.zhang@nwpu.edu.cn), [lutinglixinxin@nwpu.edu.cn](mailto:lutinglixinxin@nwpu.edu.cn);

Tel: +86 029-88460332



Que Bai

Que Bai received her BS degree from the Sichuan Agricultural University (China) in 2019. Since 2020, she has been studying for her PhD in Northwestern Polytechnical University. Her research focuses on the application of multifunctional hydrogels in wound repair.



Caiyun Zheng

Caiyun Zheng was born in Henan Province, China. She holds a master's degree in biology from Jiangsu University of Science and Technology. During her master's degree, she studied algae genetic engineering at the Institute of Oceanology, Chinese Academy of Sciences. She is currently a PhD candidate in Biomedical Engineering at Northwestern Polytechnical University. Her main research interests are porous nanomaterials, hemostatic materials, molecular biology and biochemistry.

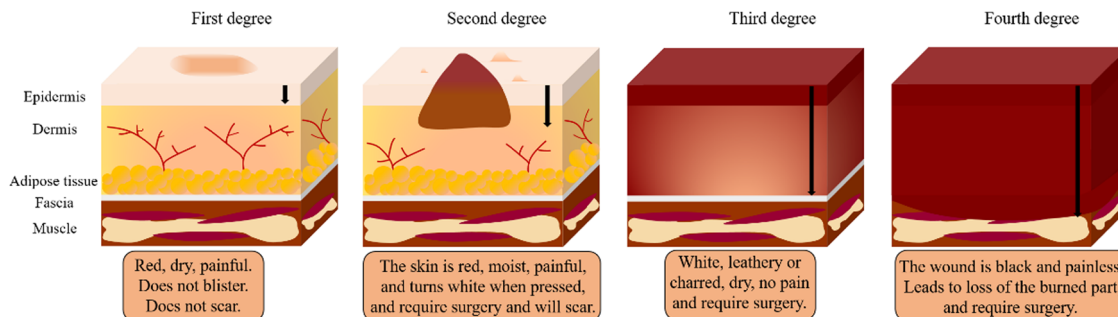


**Fig. 1** Burn depth. First-degree (superficial thickness, affecting the epidermis only) burns are typically benign, the skin turns red, very painful, heal without scarring and do not require surgery. Second degree (partial or intermediate thickness) burn causes painful blisters. The skin is red, moist, painful, and turns white when pressed. Third-degree (full thickness) burns are usually white, leathery or charred, dry, painless and require surgery. Fourth-degree burns cause damage to deeper tissues, such as muscle or bone. Usually the wound is black and painless, and frequently leads to loss of the burned part, requiring surgery (such as skin grafts).

energy.<sup>4</sup> Alkaline chemicals cause acute necrosis (tissue is transformed into a liquid, viscous mass), while acidic burn causes coagulative necrosis (the architecture of the dead tissue can be preserved).<sup>4,6</sup> Electrical injuries related to the strength of the electric field (the amperes and resistance of the tissue) tend to cause more deep tissue damage than that of visible skin damage.<sup>4,7</sup>

In addition to determining the cause of burn injuries, they must be classified according to their severity (depth and size) (Fig. 1). Currently, there are four types of burns: first-degree (superficial thickness), second-degree (partial or intermediate thickness), third-degree (full thickness) and fourth-degree.<sup>4</sup> First-degree (superficial thickness, affecting the epidermis only) burns are typically benign. The burn site turns red and painful, while it can heal without scarring and do not require surgery. Second-degree (partial or intermediate thickness) burns cause painful blisters. The skin becomes red, moist, painful, and turns white when pressed. Third-degree (full thickness) burns are usually white, leathery or charred, dry, senseless (since nerves are destroyed) and require surgery. Fourth-degree burns cause damage to deeper tissues, such as muscle or bone. Usually, the wound is black and painless and frequently loses the burned part, requiring surgery (such as skin grafts).<sup>4,8</sup> Furthermore, the burn wound can be divided

into three zones according to the severity of tissue destruction and alterations in blood flow: the zone of coagulation, the zone of stasis/ischemia, and the zone of hyperaemia (Fig. 2). The coagulation zone is exposed to the greatest heat and suffers the most damage. Proteins denature above 41 °C, so excessive heat at the damaged site results in extensive protein denaturation, degradation, and coagulation, leading to tissue necrosis.<sup>9</sup> The stasis/ischemia zone is characterized by reduced perfusion and potentially salvageable tissue. In this zone, hypoxia and ischemia can lead to tissue necrosis within 48 hours after injury in the absence of intervention.<sup>10</sup> The outermost area of a burn wound is a hyperemia zone, which increases blood flow through inflammatory vasodilation and may recover unless infected or otherwise injured.<sup>5,9</sup>

The healing of burn damage is a highly coordinated biological process including four overlapping phases: haemostasis phase, inflammatory phase, proliferation phase and remodeling phase.<sup>11</sup>

### 1.1. Haemostasis

After a burn injury occurs, the body autonomically responds to minimize the damage.<sup>12</sup> In this phase, haemostasis occurs



**Tingli Lu**

*Tingli Lu is a professor at Northwestern Polytechnical University (China). She received her PhD (2007) in Materialogy from Northwestern Polytechnical University, China. Since 2013, she has been working at the School of Life sciences, Northwestern Polytechnical University. Her research focuses on biological 3D printing, self-healing hydrogels, and medicinal carrier materials.*

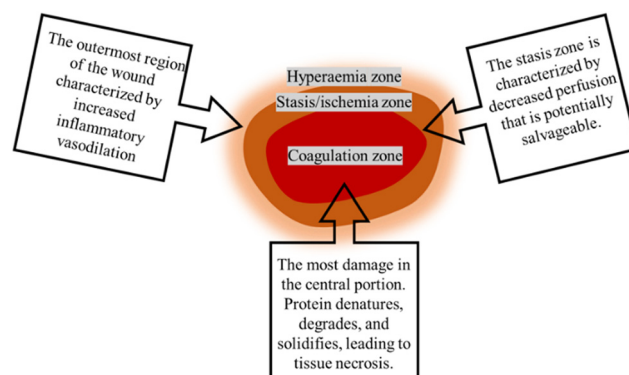


**Fig. 2** Zones of burn injury. The coagulation zone is exposed to the greatest heat and suffers the most damage. The stasis/ischemia zone is characterized by reduced perfusion and potentially salvageable tissue. Hyperemia zone that increases blood flow through inflammatory vasodilation and may recover unless infected or otherwise injured.



immediately after the injury. It involves vasoconstriction, platelet activation and aggregation, immune activation, blood clotting, complement system activation, and release of clotting and growth factors (such as platelet-derived growth factor, PDGF; epidermal growth factor, EGF; and transforming growth factor- $\beta$ , TGF- $\beta$ ) by platelets, keratinocytes, macrophages and fibroblasts. This causes the fibrin clot to deposit at the injury site as a temporary matrix for the subsequent healing phase.<sup>3,4,12</sup>

### 1.2. Inflammation

Inflammation begins within 24 hours of the burn wound. Monocytes (and macrophages) and neutrophils are recruited to the site of injury due to localized vasodilation. Three days after the initiation of injury, monocytes transform into macrophages. Neutrophils produce tumor necrosis factor (TNF- $\alpha$ ), interleukin-1 (IL-1) and interleukin-6 (IL-6), which activate inflammatory responses and stimulate the secretion of vascular endothelial growth factor (VEGF) and interleukin-8 (IL-8) to repair blood vessels.<sup>3,4,13</sup> Macrophages produce TGF- $\alpha$  and TGF- $\beta$ , fibroblast growth factor (FGF), PDGF, and VEGF to stimulate cell expansion and migration, as well as removing debris and pathogens from the site of injury.<sup>14</sup>

### 1.3. Proliferation

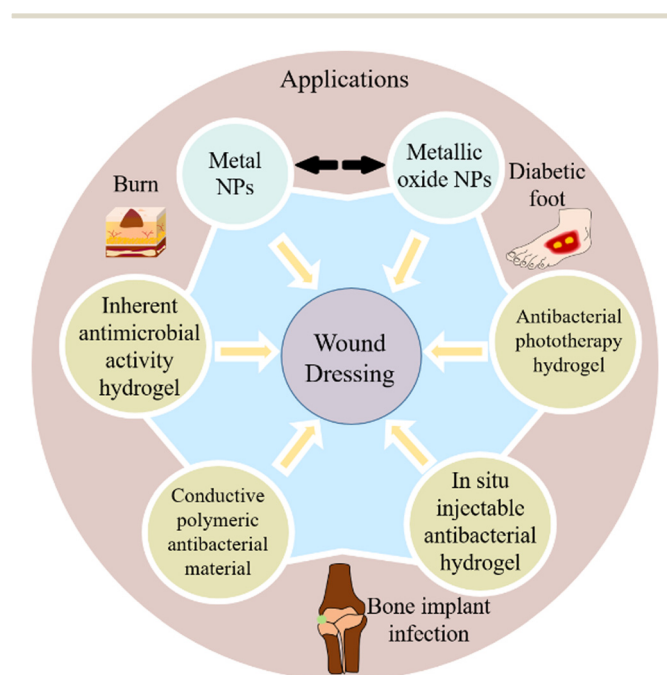
Proliferation phase consists of three steps: re-epithelialization, angiogenesis, and formation of granulation tissue. Re-epithelialization is induced by the activation of cytokines and growth factors, including insulin-like growth factor (IGF-1), nerve growth factor (NGF), EGF, and keratinocyte growth factor (KGF), which cause proliferation of keratinocytes, epithelial cells, stem cells, and fibroblasts. Keratinocytes contribute to epithelialization (wound surface closure) and angiogenesis (restoration of blood flow), and some fibroblasts differentiate into myofibroblasts, fibroblasts and myofibroblasts then produce extracellular matrix (ECM).<sup>12,15</sup> The formation of new blood vessels (angiogenesis) involves several growth factors, such as VEGF, PDGF, FGF- $\beta$ , granulocyte-macrophage colony stimulating factor (GM-CSF) and thrombin (which are the most important activators of endothelial cell growth).<sup>12,16</sup> Fibroblasts are the major cell type involved in the granulation stage, which produce collagen and other ECM molecules.<sup>17</sup> The ECM provides an appropriate scaffold for cell adhesion and organizes the growth and differentiation of cells. At the end of this stage, fibroblasts differentiate into myofibroblasts (forming a scar) or undergo apoptosis.<sup>18</sup>

### 1.4. Remodeling

During the remodeling stage, granulation tissue matures, scar tissue produces more collagen and elastin, and fibroblasts mature into myofibroblasts. The ECM is remodeled under the influence of growth factors, matrix metalloproteinases (MMPs), and tissue inhibitors of metalloproteinases (TIMPs), which results in increased tensile strength.<sup>14,19</sup>

Burn victims are at a high risk of infection, particularly drug-resistant infections, which often results in significantly longer

hospital stays, delayed wound healing, higher costs and higher mortality.<sup>20–22</sup> Therefore, the prevention and control of infection is the primary problem in the treatment of burn patients. Some routine treatments are based on the application of topical antimicrobial substances, such as topical antibiotics, povidone-iodine, silver sulfadiazine, chlorhexidine, mafenide acetate, *etc.*<sup>23,24</sup> However, the conventional treatment also faces other problems, such as solubility, overdose, and cytotoxicity. Therefore, developing an efficient and safe drug delivery system, which can reduce the risk of drug-bacterial resistance and regulate the toxicity of antimicrobial agents, is very necessary for burn infection.<sup>25,26</sup> In recent years, antibacterial nanomaterials and hydrogels have been favored by researchers. As an advanced delivery carrier, nanomaterials can be used as cell therapies, growth factors transport, gene therapy vectors, advanced antibacterial agents and biomaterials to promote wound healing.<sup>27</sup> Hydrogels are 3D porous materials that consist of physical or chemical crosslinked polymer chains.<sup>28,29</sup> Hydrogels can be developed for antibacterial applications due to their unique properties (such as hydrophilicity and porosity). In addition, some types of hydrogels have inherently antibacterial properties. In this review, we discuss the applications, challenges, advances, and new strategies of antimicrobial materials in burn treatment, and an emphasis on burn wounds, antimicrobial nanomaterials and hydrogels (Scheme 1).



**Scheme 1** Application of antimicrobial agents and antimicrobial hydrogels in wound dressings. Nanoparticles (including metals and metallic oxides) and antimicrobial agents (including antibiotics, antimicrobial peptides, antimicrobial drugs and biopolymers) in wound dressings; and hydrogels (including inherently antibacterial active hydrogels, conductive polymeric antibacterial hydrogels, *in situ* injectable hydrogels, and antibacterial phototherapy hydrogel) for burns, bone implant infections, and diabetic foot.



## 2. Application of antimicrobial agents in burns

### 2.1. Metal/metal oxides

In burn, commonly used metal/metal oxides include silver, gold, zinc oxide and titanium dioxide, *etc.* metal/metal oxides demonstrate a wide diversity of tunable properties that not only enhance their antibacterial properties, but also maintain their antibacterial activity over a long time, thus reducing the possibility of bacterial resistance.<sup>26,30</sup> Fig. 3 illustrates the possible antimicrobial mechanisms of metal/metal oxides.<sup>31</sup>

#### 2.1.1. Metal

**Silver.** Since ancient times, silver has been used in various forms, such as metallic silver, silver nitrate, silver sulfadiazine for treating infections in burns.<sup>32,33</sup> Silver has a wide antimicrobial spectrum and is effective against various aerobic, anaerobic, Gram-positive, Gram-negative, fungus and viruses.<sup>34,35</sup> The mechanism of silver ion ( $\text{Ag}^+$ ) may involve binding to the bacterial cell membrane through the interaction between  $\text{Ag}^+$  and the thiol group in proteins on the cell membrane, thus affecting the viability of bacterial cells by inhibiting DNA replication (Fig. 3(A)).<sup>31</sup>

Dressings containing silver nanoparticles have been widely used to reduce the risk of wound infection and kill bacteria in infected wounds, thus accelerating the wound healing process.<sup>36–38</sup> But silver nanoparticles cannot be directly used for biomedical applications because of their cytotoxic effects on living systems.<sup>39</sup> Therefore, silver nanoparticles should be incorporated into a polymer matrix to slow their release, reduce toxicity, and avoid penetration into other biological systems.<sup>40</sup> Batool *et al.* synthesized green silver nanoparticles through plant extracts, and this silver nanoparticle was introduced into a polymer blend (starch and polyvinyl alcohol) to form nanocomposite films. The film shows excellent physical and antibacterial properties and has great potential for application in wound dressings.<sup>40</sup> In another study, Chen *et al.* used a physical method to fabricate ultrasmall silver particles (nanoscale) and added silver particles into the carbomer gel (L-AgAPs-gel). L-AgAPs-gel (compared with commercial silver nanoparticles gels) demonstrated the broad-spectrum antibacterial activity

and prevented bacterial colonization. It was distributed locally in the skin without inducing systemic toxicities and without obvious toxicity to wound healing related cells. It can also reduce inflammation, and accelerate diabetic and burn wound healing. In conclusion, L-AgAPs-gel is an effective and safe antimicrobial and anti-inflammatory material for wound treatment, which has excellent application prospects in the future.<sup>38</sup> Yadollahi *et al.* prepared carboxymethyl cellulose nanocomposite hydrogel and combined it with silver nanoparticles to prepare antibacterial hydrogel. The antibacterial activity of the hydrogel was stable for more than one month, and it had an outstanding antibacterial effect against *E. coli* and *S. aureus*.<sup>41</sup> Later, Kim *et al.* introduced silver oxide nanoparticles into the injectable methylcellulose hydrogel, and during the process of gelation, silver oxide nanoparticles were synthesized *in situ* and evenly distributed in the gel network. The hydrogel showed excellent antibacterial activity and a significant repair effect on burn.<sup>42</sup>

Besides using silver nanoparticles as antibacterial matrices alone, it can also be combined with other substances to promote wound healing, such as graphene, polydopamine and catechin.<sup>35,43–45</sup> For example, compared with Ag NPs alone hydrogels, the Ag/graphene composite hydrogels have excellent biocompatibility, high swelling rate and good extensibility. At the same time, the hydrogels also have significant antibacterial activity and can accelerate the healing rate of rat wounds.<sup>35</sup> Furthermore, Zhou and co-workers developed a novel Ag-based bactericide (ultrafine silver/silver chloride anchored on reduced graphene oxide, Ag/AgCl/rGO). This stable Ag/AgCl nano photocatalyst can ignore the release of  $\text{Ag}^+$ , produce a high amount of oxidative radicals and kill the bacteria, and thus accelerate the epidermis regeneration and wound healing of burn wounds.<sup>43</sup> To improve the biocompatibility of AgNPs *in vivo*, Jiji *et al.* used a facile, simple catecholic redox method to anchor silver nanoparticles in bacterial cellulose (BC-PDAG), thus improving the security of silver nanoparticles. BC-PDAG nanocomposites exhibited antibacterial effects for both Gram-positive and Gram-negative bacteria. They also significantly promoted fibroblasts proliferation, granulation tissue formation, angiogenesis and re-epithelialization.

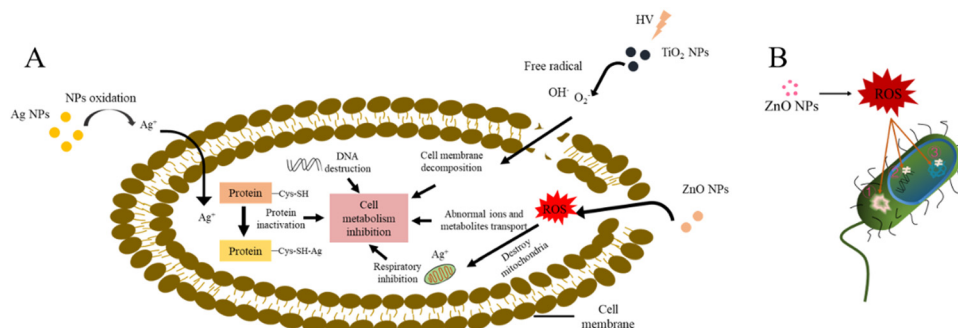


**Fig. 3** Antibacterial mechanisms of metal and metallic oxide nanoparticles. (A) Antibacterial mechanism of metal nanoparticles ( $\text{Ag}^+$ ) and metallic oxide nanoparticles ( $\text{TiO}_2$ ,  $\text{ZnO}$ ). (B) The antibacterial mechanism of  $\text{ZnO}$ . (1) Disruption the plasma membrane permeability to make some substances flow out; (2) inhibition of DNA replication; (3) protein denaturation.



Overall, BC-PDAG nanocomposites are beneficial to burn wound repair.<sup>44</sup> Kalirajan *et al.* developed bioengineered collagen scaffolds incorporated with silver–catechin nanocomposites. The scaffold has good enzymatic and thermal stability, angiogenic and antibacterial properties, and adequately promotes scarless healing in severely infected burn wounds.<sup>45</sup>

Although AgNPs have excellent antibacterial effects, the development of NPs has been largely limited due to their physical and chemical instability.<sup>26</sup> Moreover, Ag ions are efficient bactericides at a concentration of as low as  $\approx 0.001$ – $0.05$  ppm. Still we should further discuss their tissue toxicity and cytotoxicity. Furthermore, the negative impacts of AgNPs on genes need to be considered.<sup>26</sup> Therefore, toxicity should be minimized when designing AgNPs-based dressings. At the same time, green and environment-friendly AgNPs dressings should be developed, as well as stabilize and prolong the antibacterial effect of AgNPs to prevent infection and inflammation. The ability of bacteria to develop resistance to antibiotics, which limits the effectiveness of antibiotics in the treatment of infectious diseases.<sup>46</sup> So far, there have been no conclusive reports on the development of bacterial resistance to Ag NPs. However, whether silver nanoparticles can be used in medicine to enhance the effectiveness of antibiotics or completely replace them to treat local and systemic infections remains to be studied.<sup>47</sup>

**Gold.** Gold NPs (AuNPs) are widely used in tissue repair due to their easy synthesis, nontoxicity, adjustable size and shape, flexible surface modification, and tunable optical and electronic properties.<sup>48–50</sup> For example, Wei *et al.* prepared dual-functional AuNPs to treat multidrug-resistant (MDR) bacterial wounds infected by MRSA in diabetic (db/db) mice.<sup>51</sup> The antibacterial activity of AuNPs was mainly as follows: the adhesion of AuNPs to the bacterial membrane, the subsequent change of membrane potential and the decrease of ATP level, and the inhibition of tRNA binding to ribosomes.<sup>52</sup>

Yang and co-workers reported that a small molecule (6-aminopenicillanic acid, APA) coated AuNPs, AuNPs were doped into an electrospun fiber of poly( $\epsilon$ -caprolactone) (PCL)/gelatin to produce a material that prevents wound infection by MDR bacteria. Yang used small molecules that serve as the main structural components of  $\beta$ -lactam antibiotics, such as 6-aminopenicillanic acid (6-APA), 7-aminocephalosporanic acid (7-ACA), and 7-aminodesacetoxycephalosporanic acid (7-ADCA) to modify the surfaces of AuNPs. The antimicrobial activity of Au\_APA was better than that of Au\_ACA and Au\_ADCA. The antimicrobial mechanism of Au\_APA was that it could induce cell membrane rupture and bacterial cell lysis. In addition, Au\_APA NPs were non-toxic to cells at the concentration of  $20 \mu\text{g mL}^{-1}$  (8 times minimal inhibitory concentration) and showed excellent biocompatibility.<sup>53</sup> Recently, Qiao *et al.* proposed a composite structure of a cupriferous hollow nanoshell (AuAgCu<sub>2</sub>O NS), consisting of a hollow AuAg core and a Cu<sub>2</sub>O shell. On the one hand, the synergistic effect of controlled photothermal therapy and the release of silver ions from the hollow AuAg core can eradicate multi-drug-resistant bacteria,

including extended-spectrum  $\beta$ -lactamase *Escherichia coli* (ESBL *E. coli*) and MRSA. On the other hand, copper ions released by Cu<sub>2</sub>O shells can promote endothelial cell angiogenesis and fibroblast cell migration, thus enhancing wound healing.<sup>54</sup>

Au NPs appear safer for mammalian cells than other metal NPs because their antimicrobial activity is independent of reactive oxygen species (ROS). In addition, the high functionalization capabilities of these Au NPs makes them ideal nanomaterials for targeted antimicrobial applications.

**2.1.2. Metallic oxide.** Photocatalysis is the primary antibacterial mechanism of metallic oxide NPs: under the ultraviolet irradiation of sunlight, a large number of free radicals (such as hydroxyl radicals and oxygen radicals) are generated on the surface of metallic oxide NPs. When the free radicals are exposed to microorganisms, the organic matter of microorganisms are oxidized into carbon dioxide, so metallic oxide NPs can kill microorganisms in a relatively short time.<sup>26,55</sup>

**ZnO.** Zn<sup>2+</sup> is widely used as an antimicrobial agent due to its low toxicity and high biosafety.<sup>56,57</sup> However, the disadvantages of discoloration, narrow antibacterial spectrum, poor long-term durability, poor heat resistance and stability have hindered their further development.<sup>56</sup> In contrast, nanomaterials such as zinc oxide (ZnO) nanoparticles can overcome these problems to a certain extent.<sup>56,58,59</sup> ZnO is widely used in solar energy conversion, antibacterial agents and photocatalysis degradation of environmental pollutants.<sup>60–63</sup> Moreover, ZnO has unique properties that improve epithelial formation, enhance local defense systems, and reduce bacterial infection (kill bactericidal by the generating of ROS) and inflammation, thereby accelerating wound repair.<sup>64</sup> The damage mechanism of ROS to bacteria can be mainly concluded into two pathways: (1) destroying the plasma membrane permeability to make some substances flow out, or affecting the metabolic activities of the bacteria; (2) breaking and disaggregating DNA strands, generating stable oxidation products (Fig. 3(B)).<sup>56,65–67</sup> In addition, the release of Zn<sup>2+</sup> from ZnO can promote the production of fibroblasts, which is essential for the proliferation and differentiation of myofibroblasts in the dermis during skin regeneration.<sup>68–70</sup> Hadisi *et al.* prepared ZnO-containing hyaluronic acids-silk fibroin wound dressings, with the increase of ZnO content, the antibacterial activity of wound dressings against *E. coli* and *S. aureus* was enhanced, but a high concentration of ZnO (> 3%, wt%) was toxic to cells. In addition, the dressings significantly reduced inflammatory response at the wound site, promoted burn wound healing and skin regeneration (stimulated epidermis, hair follicles, sebaceous glands, and promoted collagen deposition).<sup>64</sup> Wang *et al.* used leaf extract of *Coleus amboinicus* to prepare ZnO nanoparticles, which showed excellent antibacterial activity against a variety of Gram-positive and Gram-negative bacteria, and could promote the healing of infected burns.<sup>71</sup> Thanusha *et al.* synthesized ZnO composite scaffolds to reduce inflammation and increase tissue remodeling in second degree burn healing.<sup>72</sup>

In recent years, with the development of nanotechnology, the synergistic effect of coupling hybrid nanomaterials



(bimetallic and multimetallic) to improve the antibacterial activity of nanomaterials has become a research hotspot.<sup>56</sup> For instance, Li *et al.* reported a bimetallic  $\text{CuCo}_2\text{S}_4$  NPs, which showed intrinsic peroxidase-like activity and could convert  $\text{H}_2\text{O}_2$  into  $\cdot\text{OH}$  at neutral pH.  $\text{CuCo}_2\text{S}_4$  NPs could effectively destroy MRSA biofilms *in vitro* and promote burn healing of MRSA infection *in vivo*.<sup>73</sup> Wang *et al.* prepared a hybrid multi-shelled hollow materials by coupling CuO and ZnO NPs with AuNPs ( $\text{ZnO@CuO@Au}$  NPS). Due to the combined action of PTT, PDT,  $\text{Zn}^{2+}$  and  $\text{Cu}^{2+}$  under 635 nm laser irradiation, it showed significant antibacterial effect against *S. aureus* (99.80%) and *E. coli* (97.5%) within 10 min after application.<sup>56</sup>

**$\text{TiO}_2$ .** The super-hydrophilic, photocatalytic properties, stable chemical properties and excellent biocompatibility of titanium dioxide ( $\text{TiO}_2$ ) NPs make them ideal candidates for the pharmaceutical industry, especially in bone tissue engineering nano- $\text{TiO}_2$  bone scaffolds, biosensors and vascular implant manufacturing.<sup>74</sup> In addition, the photocatalytic activity of  $\text{TiO}_2$  NPs makes the surface have antimicrobial properties under UV irradiation.<sup>75</sup> Ismail *et al.* mixed  $\text{TiO}_2$  NPs into Gellan gum (GG) bipolymer to enhance its mechanical properties, antibacterial properties and biocompatibility. The results showed that the GG +  $\text{TiO}_2$ -nanobiofilm had antibacterial activity (the inhibition zone against *S. aureus* and *E. coli* was  $9 \pm 0.25$  mm and  $11 \pm 0.06$  mm, respectively, which was similar to that of the penicillin control sample), promoted cell proliferation and growth, and facilitated wound healing.<sup>76</sup> However,  $\text{TiO}_2$  has the photocatalytic activity of producing ROS, while the recombination of generated electrons and holes limits its photocatalytic performance and reduces its actual antibacterial effect.<sup>77</sup> Recently, researchers have loaded antibiotics, metal NPs, and other antimicrobial elements onto  $\text{TiO}_2$  surfaces for antimicrobial applications.<sup>78,79</sup> However, bacterial resistance caused by the antibiotic application and the potential cytotoxicity of metal NPs limits their clinical application. Therefore, Wang *et al.* used electrostatic force to assemble graphdiyne (GDY) onto  $\text{TiO}_2$  to combat implant infection by enhancing photocatalysis and prolonging antimicrobial activity. The nanofibers

exhibited excellent photocatalytic performance and increased the production of photocatalytic ROS. The resulting ROS induces oxidation of cell components and perforation of bacterial cell walls, leading to membrane leakage, structural destruction, and ultimately bacterial death.<sup>77</sup>

In addition,  $\text{TiO}_2$  is also widely used in burn repair.<sup>80</sup> For example, Seisenbaeva *et al.* produced  $\text{TiO}_2$  through the hydrolysis pathway of triethanolamine ligands modified  $\text{TiO}_2$ , and the interaction between human blood and  $\text{TiO}_2$ , resulted in the formation of reasonably dense gel composites materials. The composite material can prevent skin infection and inflammation and accelerate wound healing in burned rats.<sup>81</sup> Kalirajan *et al.* explored the *in vivo* burn wound healing potential of  $\text{TiO}_2$  and bacterial cellulose (BC) nanocomposite ( $\text{BC-TiO}_2$ ). First, the physicochemical characterization of  $\text{BC-TiO}_2$  was characterized by SEM, XRD and FTIR. Second, antimicrobial experiments showed that the  $\text{BC-TiO}_2$  nanocomposite produces highly reactive species that disrupt the lipopolysaccharides and peptidoglycan components of cell membranes, thereby inducing cell death, which is consistent with earlier reported literature.<sup>82</sup> Furthermore, the wound area and histopathology in the burn wound model were used to evaluate the healing effect of  $\text{BC-TiO}_2$  nanocomposites *in vivo*. In summary,  $\text{BC-TiO}_2$  nanocomposite dressings provide a sterile and favorable environment for skin repair.<sup>80</sup>

In another study, Zhang *et al.* prepared yolk-shell particles (YSPs) using trineedle coaxial electrospraying with a simple nonsolvent process (Fig. 4). Among them,  $\text{TiO}_2$ -Ag NPs and ganoderma lucidum polysaccharides as the main antibacterial and antioxidant components were encapsulated into the outer shell of YDPs, and iron oxide ( $\text{Fe}_3\text{O}_4$ ) NPs were combined into the inner core as a photothermal agent. Cell experiments showed that YSPs had good biocompatibility and antioxidant activity. The antibacterial test showed that YSPs had significant antibacterial activity against *E. coli* and *S. aureus*. *In vivo* burn wound healing in c57 mice demonstrated that the YSPs had low biological toxicity and could promote wound healing in some ways.<sup>83</sup>

Mesoporous silica NPs have good biocompatibility and have been used as promising drug and gene carriers.<sup>84</sup> In addition,

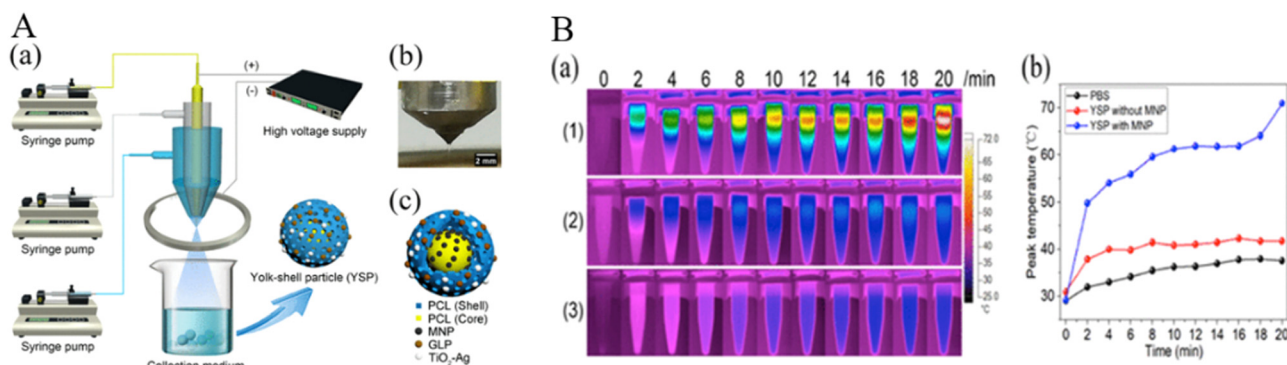


**Fig. 4** (A) (a) Schematic illustrations of the trineedle coaxial electrospraying system and collection system. (b) Digital graph of the stable jetting mode. (c) Schematic illustration of the structure of the YSPs. (B) (a) Thermal graphs of the sample in EP tubes at determined time points (b) Peak temperature rise curves of the sample EP tubes of three groups. (1) YSP with MNP and  $\text{TiO}_2$ -Ag group, (2) YSP containing  $\text{TiO}_2$ -Ag without MNP group, (3) PBS group.<sup>83</sup> Copyright 2013, ACS Publications.

the silica NPs show high chemical stability, and the surface can be easily modified.<sup>85</sup> The increased surface area combined with the pore distribution makes the therapeutic agents easy to load. Studies of SiO<sub>2</sub> have shown that they are non-toxic and can be used for *in vivo* and biomedical applications.<sup>86,87</sup> Kalirajan *et al.* prepared a hybrid scaffold of collagen, which was combined with a silica-resorcinol composite (Si@Res) to improve bio-availability and achieve better healing. The hybrid biomaterials have good biocompatibility for the blood cells and keratinocytes and have an excellent antibacterial property. *In vivo* results suggest that Si@Res composite contributes to scar-free wound healing (type I diabetes and chronic infectious burns in rats) by increasing TGF- $\beta$ 3 expression.<sup>88</sup>

Metal/metal oxides nanomaterials have good antibacterial and wound healing ability, and there is still great application and development potential in the future. However, it should be noted that metal/metal oxides nanomaterials are in direct contact with tissue in the wound, and the biosafety of the products must be considered before application. The metal/metal oxides nanomaterials can contact with blood cells in the blood vessels of the wound and enter the blood circulation. This phenomenon can cause hemolysis. Some metal/metal oxides nanomaterials, such as AgNPs and ZnO NPs, have been found to cause hemolysis. So we can adjust the physical and chemical properties of the material, or wrap biologically active substances such as polysaccharides onto the surface of the nanomaterials.

## 2.2. Antimicrobial agents

**2.2.1. Antibiotics.** Burn wound associated infection is one of the severe complications in the acute period after burn injury, and it is estimated that approximately 45% of post-burn mortality is associated with infection, such as those caused by *P. aeruginosa* or MRSA.<sup>89,90</sup> The formation of infection can severely impair the proliferation of dermal cells, resulting in degeneration of the surface layer and part of the thickness to more profound tissue damage, thereby limiting dermal regeneration.<sup>91</sup> Antibiotics are widely used in the treatment and repair of burn infection.<sup>92–94</sup>

**Tetracycline.** Tetracycline (TC) is one of the most effective antibiotics against bacterial infections, such as acnes, periodontal and urinary.<sup>95</sup> In addition, TC has fluorescence properties, which is helpful to evaluate drug diffusion characteristics.<sup>96</sup> Chen *et al.* prepared citric modified chitosan (CC) hydrogel containing the antimicrobial drug TC. The cumulative release of the drug was regulated by CC concentration, and the drug-loaded CC hydrogels showed enhanced antimicrobial activity against *E. coli* and *S. aureus*. In animal experiments, CC hydrogels loaded with TC accelerated wound healing in rats.<sup>97</sup>

In one study, Saito *et al.* loaded TC into nanosheets to evaluate the antimicrobial properties of the nanosheets in mice that were burned and infected with *P. aeruginosa*. By analyzing the viable count of bacteria at the wound site, histology and the amount of bacteria in the liver showed that the nanosheets had strong antibacterial activity, thus inhibiting burn infection.<sup>90</sup>

**Minocycline.** Minocycline (MC) is a broad-spectrum antimicrobial TC antibiotic than other family members (especially for burn wounds).<sup>98,99</sup> MC is effective against both Gram-positive and Gram-negative bacteria and prevents cell death and increases cell proliferation in wound repair.<sup>100</sup> Various drug delivery systems have been investigated to apply MC to burn wound healing.<sup>101,102</sup> For instance, Mohebbi *et al.* prepared a novel wound dressing based on nanocomposite film of polyvinyl alcohol (PVA) and halloysite nanotubes (HNT) loaded with MC. Drug release studies showed that the drug was slowly released from the nanocomposite and in accordance with the Korsmeyer-Peppas model.<sup>101</sup> In addition, nanocomposites have antimicrobial effects against both Gram-positive and Gram-negative bacteria and can promote burn wound repair (Fig. 5).<sup>101</sup> Recently, a layered biocompatible pH-sensitive antimicrobial composite membrane based on Halloysite nanotube/poly(lactic-co-glycolic acid)/chitosan (HNT/PLGA/chitosan) was prepared for the controlled release of MC on burn wounds.<sup>103</sup> HNT composites were modified with different concentrations of PLGA and chitosan by a layer-by-layer strategy. Firstly, HNT lumens were etched with sulfuric acid to increase drug loading efficiency (base spacing is increased by dimethyl sulfoxide intercalation). Then, the outer surface of HNT was modified with APTES silane reagent. Subsequently, a PLGA coating was produced on modifying HNT using an LBL strategy and the solid-in-oil-in-water (s/o/w) emulsion system. Finally, the prepared HNT/PLGA suspension was coated with chitosan under acidic conditions. The results showed that the release of MC was slow and controlled. In addition, compared with pure HNT, the load of MC on etched intercalated HNT films increased by about twice, and both Gram-positive and Gram-negative bacteria were inhibited. The composite membrane loaded with MC can significantly promote the healing of burn wounds in rats.

In another study, Kaur *et al.* used a polyvinyl alcohol-sodium alginate (PVA-SA) hydrogel wound dressing system for topical delivery of MC to treat infected burns.<sup>104</sup> The cytocompatibility and antibacterial properties of hydrogels were evaluated by *in vitro* antibacterial assays, elution assays and cytotoxicity tests. After 24 h incubation of RAW 264.7 macrophage cell lines and SK-1 skin epithelial cell lines with PVA-SA hydrogel extracts, the average cell viability of RAW 264.7 and SK-1 was 94.25% and 95.4% respectively. The results showed that the PVA-SA hydrogel had good cytocompatibility and could be used for further experiments *in vivo*. The zone of inhibition assay showed that a clear inhibition zone was observed around the PVA-SA film coated with MC. The elution profile showed that 99.9% of antibiotics were released within the first 15 minutes. In summary, PVA-SA membranes can be used as commercial wound dressings to deliver novel antimicrobial compounds against antibiotic-resistant pathogens in localised infection situations.

**Gentamicin.** Gentamicin is a traditional broad-spectrum aminoglycoside antibiotic used to treat skin, soft tissue and wound infections, such as, chitosan containing gentamicin nano-biocomposite membrane to accelerate wound repair.<sup>26,105</sup>



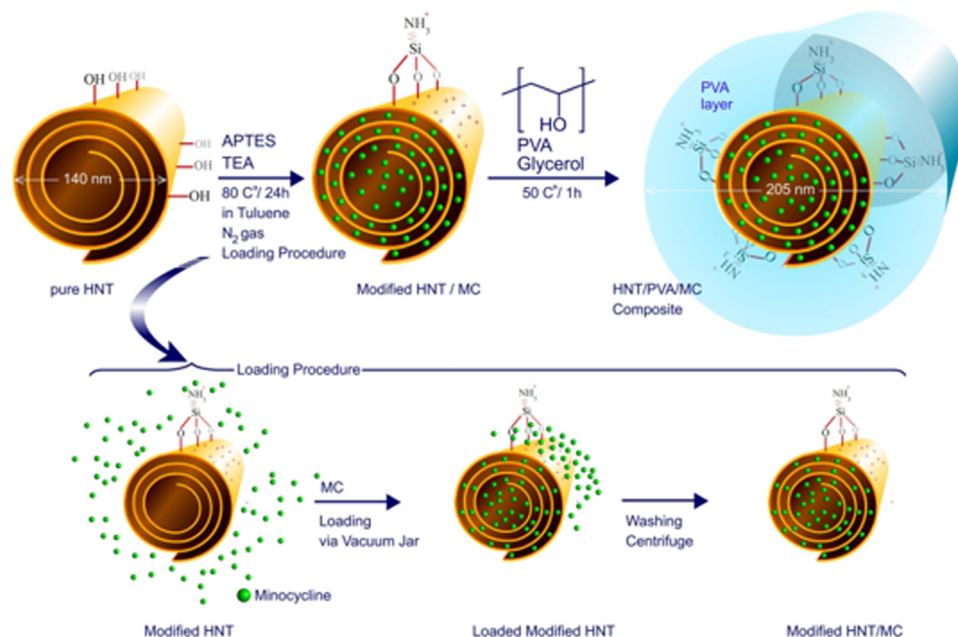


Fig. 5 Schematic of surface modification and synthesis of HNT/PVA nanocomposites and drug loading within the HNT lumen. Add HNT to the toluene and stir. Then, TEA and APTES were added to the obtained suspension, and the mixture was refluxed at 80 °C in a nitrogen atmosphere for 24 h to obtain HNT-APTE. The minocycline molecules in its saturated solution are loaded with pH control into the HNT lumen, and the material is added to PVA hydrogels and glycerol and cast as a film.<sup>101</sup> Copyright 2020, Elsevier.

In another study, Lan and his team impregnated gelatin microspheres (GMs) with the antibiotic gentamicin sulfate (GS) and then embedded the GMs in a silk fibroin (SF) to fabricate GS/GM/SF scaffolds. GS/GM/SF scaffolds not only significantly reduced the burn infection of *P. aeruginosa*, but also accelerated the regeneration of dermis.<sup>106,107</sup>

In another study, Zilberman *et al.* developed a double-layer wound dressing with a top layer of gentamicin-containing porous poly(DL-lactic acid-co-glycolic acid) to prevent and/or fight infection, and a bottom layer of spongy collagen designed to maintain high absorbability of wound exudates and to accommodate newly formed tissue.<sup>108</sup> Three different gentamicin-loaded emulsions (BSA, SPAN and BSA2) were used to study drug release kinetics. BSA samples usually showed a relatively high burst release of gentamicin ( $38.4 \pm 4\%$ ), followed by a release of 80% within 4 days. SPAN formulation had a lower burst release rate ( $8.2 \pm 2\%$ ), with a total release of 84 days. BSA2 agents exhibited intermediate drug release behavior (medium burst release and medium release rate). In addition, second-degree burns in guinea pigs were used as a wound-healing model to test the healing potential of hybrid wound dressings. *Pseudomonas* was applied topically immediately after the infliction of the burns to mimic burn contamination that typically occurs in patients with burns. Results showed that the hybrid dressing loaded with gentamicin significantly accelerated wound healing (28%), which is at least double that obtained by the Melolin<sup>®</sup> and Aquacel<sup>®</sup> Ag formats (8–12%). The dressings also promoted angiogenesis, epithelialization, collagen formation, and reduced mononuclear infiltration at the wound site. In short, gentamicin-slow releasing hybrid dressing materials

offer a potentially valuable and economical method for treating life-threatening complications of burn-related infections.<sup>108</sup>

In addition, datoromycin is a novel cyclic lipopeptide antibiotic with selective activity against aerobic, anaerobic and facultative Gram-positive bacteria.<sup>109,110</sup> Simonetti *et al.* treated burn wounds caused by MRSA infection with datoromycin.<sup>111</sup> Fusidic acid (FA) is an antibiotic derived from the fungus *Fusicidium coccineum*, belonging to the BCS 3 category. FA blocks bacterial protein synthesis by binding to EF-G on bacterial ribosomes, thus inhibiting bacterial translation.<sup>112</sup> Thakur *et al.* combined FA with lipid-polymer hybrid NPs (LPHNs) to treat of MRSA-infected burn wounds.<sup>113</sup>

Although antibiotics plays an essential role in the treatment of infections, however, antibiotic drug-resistant bacteria is inevitable. The emergence of antibiotic resistance can be attributed to several reasons.<sup>114</sup> First, bacteria are unicellular micro-organisms, and their reproduction can occur rapidly through binary division.<sup>115</sup> In addition, their small size increases the chance of local population variation, which leads to continued growth and evolution, and increased adaptability against antimicrobial agents.<sup>116</sup> Furthermore, the cost of survival for maintaining this evolutionary resistance has proven to be low because antimicrobial organisms rarely lose resistance even in the absence of threatening agents.<sup>114</sup> Finally, traditional antibiotic treatment is associated with overprescribing and improper use, ultimately leading to a gradual rise in antibiotic resistance in a variety of pathogens.<sup>114</sup>

**2.2.2. Antimicrobial peptides.** Antimicrobial peptides (AMPs) are natural or synthetic polypeptide molecules. Most AMPs have cationic characteristics due to the prevalence of basic



residues.<sup>3,117,118</sup> AMPs, which do not easily develop drug resistance, can also be used as immunomodulating and antiviral agents. AMPs themselves represent the first line of defense against invading pathogens and are a vital part of the innate immune system of many organisms.<sup>119,120</sup> AMPs as an antimicrobial agent can destroy/kill a variety of microorganisms. The main mechanism of action is to attach and destroy negatively charged phospholipids of the microbial membrane through simple electrostatic interaction, inhibit microbial proteins and nucleic acids leading to the decomposition/perturbation of the latter, and inhibit/kill microorganisms. Therefore, they can be used to treat burn infections.<sup>3,118,121,122</sup>

More than 5000 natural and synthetic antimicrobial peptides have been discovered to date.<sup>123</sup> Natural AMPs such as bovine lactoferrin (lactotransferrin, LTF) have been introduced as potential antimicrobial agents for the treatment of infectious diseases.<sup>124</sup> LTF is a glycoprotein composed of 689 amino acid residues, which contributes to the transport and regulation of iron in cells and stimulates the proliferation of lymphocytes and the phagocytic activity of macrophages. LTF is an integral part of the human immune system.<sup>124</sup> The synthetic AMPs also showed excellent antimicrobial activity (such as against *P. aeruginosa* and MRSA).<sup>117,125</sup> *P. aeruginosa* can cause sepsis and *S. aureus* can cause chronic infection, both of which are considered to be representative pathogens involved in burn infection.<sup>126,127</sup>

*P. aeruginosa* is the most common Gram-negative bacterium on burn wounds, eventually colonizes over 70% of burn wounds. More than 95% of *Pseudomonas* organisms may be resistant to multiple antibiotics.<sup>128</sup> Therefore, inhibition of *P. aeruginosa* on burn wounds is significant to repair. For example, a short synthetic AMP, PXL150, has broad-spectrum bactericidal activity against both Gram-positive and Gram-negative bacteria, as well as *Candida* spp, and has shown anti-inflammatory properties in human cell lines.<sup>129,130</sup> Moreover, Bjorn *et al.* evaluated the anti-infective effect of PXL150 in hydroxypropyl cellulose (HPC) gel against *P. aeruginosa* infection burn mouse models *in vitro* and *in vivo* the safety of

PXL150 in rats and rabbits. The minimum concentration analysis showed that PXL150 had a significant bactericidal effect against *P. aeruginosa in vitro*. In non-clinical safety studies, PXL150 has demonstrated good safety after repeated systemic and local administration in rats and rabbits, respectively. Therefore, PXL150 has the potential to be an effective and safe drug candidate for the treatment of infected burns.<sup>122</sup> Recently, Mohamed *et al.* synthesized short  $\beta$ -sheet folding peptides (IRIKIRIK, IK8L), the IK8L can inhibit biofilm in the growth of MDR *P. aeruginosa*, and IK8L has the development tendency is lower resistance than conventional antibiotics (repeated use of IK8L does not cause drug resistance), and it has an excellent effect on the treatment of MDR *P. aeruginosa* infected burn wounds.<sup>121</sup> In one study, Pan and his team showed that unnatural amino-acid-based star-shaped poly-(L-ornithine)s have significant proteolytic stability, excellent biofilm destruction ability, and broad-spectrum antibacterial activity, especially against *P. aeruginosa*.<sup>126</sup> In a mouse model of skin burns infected with *P. aeruginosa*, star peptides can reduce the microbial burden in the infected area and promote burn healing (Fig. 6).

*S. aureus* is the most common pathogenic microorganism for skin infections and the second most common cause of hospital bloodstream infections.<sup>131</sup> *S. aureus* are resistant to all currently available  $\beta$ -lactam antibiotics, including penicillin and cephalosporin, and are commonly referred to as MRSA.<sup>132</sup> *S. aureus* and MRSA are the leading causes of morbidity in thermally injured patients.<sup>133</sup> When MRSA enters the burn wound, it may lead to serious invasive diseases, such as sepsis, endocarditis, toxic shock syndrome, and necrotizing pneumonia, by evading the body's natural protective mechanisms.<sup>134</sup> In the context of increasing antibiotic resistance, AMPs, as new anti-infective agents, have been favored by researchers due to their broad-spectrum activity, multiple action modes, rapid killing kinetics, minimal host toxicity and low sensitivity to multi-drug resistance mechanisms.<sup>135</sup> In an investigation, Ma *et al.* evaluated the effect of a novel engineered amphiphilic peptide WRL3 (WLRAFRRLLVRLARGLLRR-NH2) on burn infection with

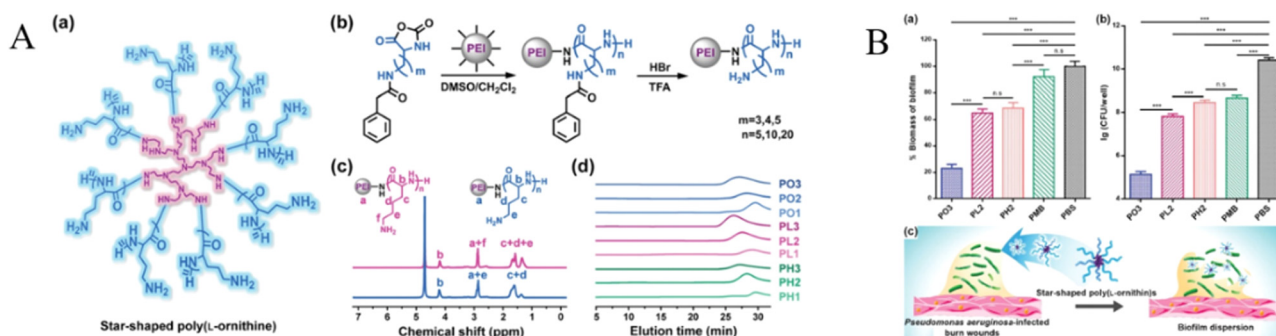


**Fig. 6** (A) (a) The structure of PEI-g-PLO. (b) Synthetic route of star-shaped polypeptides. (c) <sup>1</sup>H NMR spectra of representative star-shaped polypeptides PL2 (red) and PO3 (blue). (d) GPC chromatograms of star-shaped polypeptides. The structure of only one arm of the star-shaped polypeptide is shown in panel (b). (B) (a) Biofilm disruption of the star-shaped polypeptides. (a) Quantitative determination of the biofilm-disrupting capacity of PO3, PL2, PH2, polymyxin B (PMB), or PBS by measuring the absorbance of CV-stained biofilms of *P. aeruginosa* ( $n = 3$ ). (b) Bacterial count enumeration of *P. aeruginosa* biofilms treated with PO3, PL2, PH2, polymyxin B (PMB), or PBS ( $n = 3$ ). (c) Schematic illustration of biofilm-disrupting property of star-shaped polypeptides. \* $p < 0.05$ , \*\* $p < 0.01$ , and \*\*\* $p < 0.001$ ; n.s.: nonsignificant.<sup>126</sup> Copyright 2020, Wiley.

MRSA. Studies have shown that WRL3 may exert its bactericidal activity by destroying the bacterial membrane and promoting the healing of MRSA infections of skin burn wounds.<sup>134</sup>

In addition, Obuobi and his colleagues used the high binding affinity between polyanionic DNA nanostructures and cationic AMPs (L12 peptides) to create hydrogels.<sup>136</sup> Specific methods: using the unique self-recognition of DNA bases and the electrostatic interaction between polyanionic DNA and cationic peptides, Y-shaped nanostructured “monomers” are cross-linked with complementary sequences on the L-linker to form a physically cross-linked hydrogel network that immobilizes AMPs. *In vitro* L12 release studies showed that the DNA hydrogel was relatively stable for 24 h in the absence of DNase. In the presence of 10 U mL<sup>-1</sup> DNase I, L12 was released with a half-life of 3 h and was released entirely by 12 h before. At the concentration of 60 U mL<sup>-1</sup> DNase I, the half-life was 0.5 h, and it was wholly released in 1.5 h. In the presence of *S. aureus*, *in vitro* gel degradation test was conducted to verify the antimicrobial activity of hydrogels. The results showed that DNase was produced by *S. aureus* (ATCC 29,737) and MRSA (DR09808R) to degrade the hydrogels, followed by the release of L12, resulting in an antimicrobial effect. The system has potential applications in AMP delivery and skin wound treatment in the future.

Although AMPs are superior to antibiotics in terms of drug resistance, the clinical development of AMP drugs still has the following shortcomings: firstly, unstable proteolysis *in vivo*, low permeability across biological barriers, and significant systemic toxicity caused by non-target effects.<sup>136,137</sup> Secondly, covalent fixation of AMPs on polymer scaffolds is often limited, such as reduced antimicrobial activity, the use of toxic crosslinkers, and the characterization of covalently bound AMPs on hydrogel scaffolds is difficult to determine.<sup>138–140</sup> Furthermore, the lack of good models or evaluation methods for compound screening may be responsible for the mismatch between *in vitro* and *in vivo* efficacy.<sup>123</sup> In the future, the expanding catalogues of self-assembling protein domains, AMPs and targeting ligands, as well as newly developed nanobiotechnological approaches, are expected to lead to a new generation of rational AMPs for safer, highly efficient and more selective treatment of bacterial infections in the short term.

**2.2.3. Drugs.** Silver sulfadiazine (AgSD) is a topical antibacterial agent for burn wounds in clinical practice, which has antibacterial effect against multi-drug resistant bacteria such as MRSA.<sup>141,142</sup> Many studies have shown that AgSD-based antimicrobial materials can be used to treat burn wounds.<sup>142–144</sup> In an experiment, Ito *et al.* prepared poly(lactic acid) (PLA) nanosheets loaded with AgSD, which could slowly release Ag<sup>+</sup> ions for more than 3 days and had no significant cytotoxicity on fibroblasts at the dose of AgSD. In addition, it has shown antibacterial efficacy against MRSA *in vitro* tests. In animal studies, the nanosheets significantly reduced the number of MRSA bacteria at the injury site (more than 10<sup>5</sup> fold) and inhibited inflammation, thus speeding up the burn wound healing process.<sup>142</sup> In another experiment, Kumar loaded AgSD into the carbopol gel, reducing the toxicity of the drug

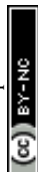
immediately released to the target area. The optimized microgel enhanced the retention of the drug in the skin layers (3 fold higher than the commercially available product). The antibacterial effect of *S. aureus* and *P. aeruginosa* was similar to that of commercial products. *In vitro* burn experiments showed that the gel containing AgSD reduced the cytotoxicity of skin cell lines and promoted the contraction of burn wound.<sup>143</sup> Recently, Thakur *et al.* have incorporated silver sulfadiazine into egg oil-organogel (SSD-EOOG) through a design quality method, the system enhances drug penetration (72.33 ± 1.73%) and retention efficacy (541.20 ± 22.16 µg cm<sup>-2</sup>). Therefore, the SSD-EOOG improves topical delivery drugs of burn wounds and patient compliance.<sup>144</sup>

**2.2.4. Biopolymers.** Biopolymers are biocompatible and can expand by absorbing liquids through their polymeric networks. Thus, they provide a suitable matrix to stimulate the healing cascade, mimicking the extracellular matrix environment in a moist medium.<sup>145,146</sup> Among various biopolymers, chitosan has been extensively used in wound healing.<sup>147,148</sup> Chitosan is a polymeric compound found in nature with good biocompatibility and biodegradation. Chitosan is a highly basic, natural, cationic and mucosal adhesion polysaccharide composed of β-1,4-linked 2-amino-2-deoxy-β-D-glucose (deacetylated D-glucosamine) and N-acetyl-D-glucosamine units, and it is a kind of a bioactive compound with a variety of biological properties, such as antifungal, antimicrobial and antioxidant activities.<sup>146,149</sup> Chitosan NPs can be generated by the complex coacervation method, ionotropic gelation, coprecipitation method, emulsification solvent diffusion and reverse micellar method.<sup>150</sup>

Recently, temperature-sensitive chitosan (TCTS) hydrogel was synthesized by β-glycerolphosphate, acetic acid and chitosan. Then, its potential for wound healing in burn patients was evaluated both *in vitro* and *in vivo* rat models.<sup>151</sup> The cytotoxicity of TCTS hydrogel was detected by human foreskin fibroblast cells (HU02). It was found that there was no significant difference in the activity of HU02 cultured on TCTS hydrogel compared with the control group. Animal experiments showed that burn wound healing, re-epithelialization and wound closure were significantly faster in TCTS hydrogel group than in the control group. In general, TCTS hydrogel is an excellent wound dressing for burn infected full-thickness wounds.

Although chitosan NPs have antibacterial effects, their exact mechanism of action is still under discussion. Various hypotheses on the mechanism of chitosan antimicrobial action: polycationic nature of chitosan, binding to bacterial DNA (inhibition of mRNA), chelation agent (nutrients and essential metals), and blocking agent (Fig. 7).<sup>152</sup>

Hypothesis 1: the interaction between positively charged chitosan molecules and negatively charged microbial cell membranes increases the permeability of the bacterial membrane, leading to leakage of intracellular components and cell death. Several research results support this hypothesis: for example, to improve the water-solubility and antimicrobial activity of chitosan, Yan *et al.* prepared a new chitosan



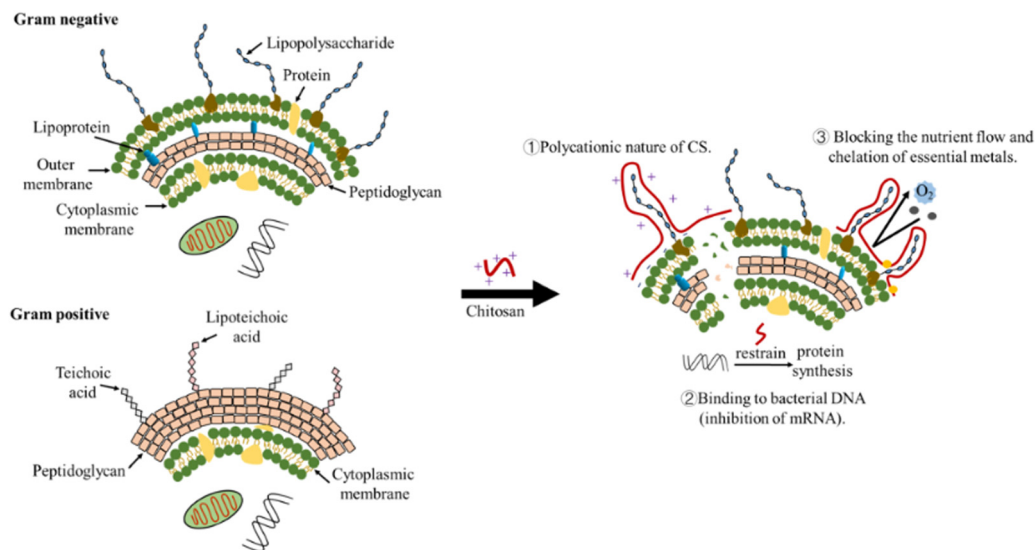


**Fig. 7** Four models of chitosan action on Gram-positive and -negative bacteria: (1) the interaction between positively charged chitosan molecules and negatively charged microbial cell membranes increases the permeability of bacterial membrane, leading to leakage of intracellular components and cell death. (2) Intracellular binding of chitosan to DNA of target microorganism inhibits mRNA activity, thereby inhibiting protein synthesis. (3) Chitosan selectively binds essential metals, thereby inhibiting microbial growth and toxin production. (4) Chitosan can form a membrane barrier on the surface of bacterial cells, preventing nutrients and oxygen from entering the bacteria, thus inhibiting bacterial growth.

derivative, 3,6-O-[N-(2-aminoethyl)-acetamide-yl]-chitosan (AACS). AACS could reduce surface hydrophobicity, cell viability, and intracellular proteins by increasing membrane permeability. The results of SEM further confirmed the bacterial membrane collapse and disruption caused by AACS.<sup>153</sup> The direct relation between chitosan antibacterial effect and its degree of deacetylation (DD) is associated with the number of its protonated amine groups.<sup>154</sup> For chitosan with DD > 81.35%, the minimum inhibitory concentrations against *E. coli* and *S. aureus* was 0.0625% and 0.0313%, respectively. For chitosan with DD = 100.00%, the minimum bactericidal concentration against both *E. coli* and *S. aureus* was 0.0156%. The antimicrobial activity of chitosan was due to the amino protonation and cationization of its molecular side chains in acidic solutions. *E. coli* and *S. aureus* were initially inhibited, and the cells were gradually broken and decomposed.<sup>155</sup> In conclusion, these findings all support the hypothesis that the antimicrobial action of chitosan is attributed to its effect on cell membranes. At present, this hypothesis is generally accepted by most researchers.

**Hypothesis 2:** intranuclear binding of chitosan to DNA of target microorganism inhibits mRNA activity, thereby inhibiting protein synthesis. Typically, chitosan of low molecular weight ( $\leq 50$  kDa) can penetrate bacterial cell walls and inhibit DNA transcription.<sup>154</sup> In a study, the chitosan-ferulic acid conjugate CFA may inhibit the mRNA expression of *mecA* gene and thus inhibit the activity of MRSA.<sup>156</sup> In another study, confocal laser microscope showed that chitooligomers down-regulated DNA in *E. coli*.<sup>154</sup> **Hypothesis 3:** chitosan selectively binds essential metals (such as  $\text{Ca}^{2+}$  and  $\text{Mg}^{2+}$ , which play an important role in bacterial metabolism), thereby inhibiting microbial growth and toxin production. The chitosan-metal complex helps to obtain a higher positive charge, which leads

to better antimicrobial activity.<sup>152,157</sup> **Hypothesis 4:** chitosan can form a membrane barrier on the surface of bacterial cells, preventing nutrients and oxygen from entering the bacteria, thus inhibiting bacterial growth.<sup>152</sup>

Currently, many studies have shown that chitosan-based NPs has a higher killing effect than chitosan alone.<sup>158</sup> For instance, Luna-Hernandez *et al.* prepared CS/nAg nanocomposites by chemical reduction method. A fixed weight of CS and various ratios of 0.01, 0.025, 0.05 and 0.1 M for silver sources were applied for preparing the CS/nAg nanocomposites. The formation of nAg was confirmed by the characterization of CS/nAg by UV-Vis and FTIR. *In vitro* antibacterial experiments showed that CS/nAg nanocomposite showed high antibacterial activity against *S. aureus* and *P. aeruginosa*. Thermal burns treated with CS/nAg nanofilms, and 7 day results showing the presence of epidermis and orthokeratosis, as well as dermal papillae and hair follicles. In addition, dense myofibroblast populations and angiogenesis can be seen, indicating that tissue damage is in a stage of proliferative and healing due to epithelial differentiation.<sup>159</sup> In another research, Abid *et al.* prepared polyethylene oxide-chitosan (PEO-CS) nanofibers and studied the rheological properties of PEO-CS and the optimized process parameters of nanofibers using response surface methodology. The PEO-CS nanofibers were successfully electrospun with a very small standard deviation at a lower voltage, and the zinc oxide-loaded nanofibers showed better thermal stability and antibacterial activity. The nanofiber is expected to be a candidate material for the prevention or treatment of burns.<sup>160</sup>

In addition, CS can also be combined with antimicrobial agents, metallic antimicrobial particles, and natural compounds to enhance the antimicrobial effect.<sup>161,162</sup> For example,



Chen *et al.* prepared hydroxylated lecithin complexed iodine/carboxymethyl chitosan/sodium alginate composite membrane (HLI/CMCS/SA) by microwave drying and explored the potential value of composite membranes as wound repair dressings using the infection of a rat model of the seawater immersed wound infection of deep partial-thickness burns.<sup>161</sup> *In vitro* antibacterial experiments showed that HLI/CMCS/SA composite membranes could effectively inhibit Gram-positive bacteria (*Staphylococcus aureus* and *Enterococcus faecalis*) and Gram-negative bacteria (*Pseudomonas aeruginosa*, *Escherichia coli*, *Acinetobacter bauman* and *Vibrio vulnificus*). Animal experiments showed that the wound healing rate of the HLI/CMCS/SA composite membranes group was higher than that of the control group at the 4 th, 8 th and 16 th days, indicating that the composite membranes could effectively promote the healing of the seawater immersed wound infection of deep partial-thickness burns. Seawater soaked wounds are susceptible to infection by Gram-negative bacteria.<sup>163</sup> Therefore, HLI/CMCS/SA composite membranes can be used as a repair dressing for seawater immersed wounds. In another work, Kamakshi and his team modified acellular dermal matrix (ADM) by a dual cross-linking method called CSADM-Cl (using chitosan for ionic cross-linking and an iodine-modified 2,5-dihydro-2,5-dimethoxyfuran cross-linking agent for covalent cross-linking). CSADM-CL has good antibacterial activity and angiogenic ability. In addition, CSADM-CL can treat full-thickness burns and shows rapid healing characteristics.<sup>162</sup>

Although CS has significant antimicrobial activity against various fungi and bacteria, the following problems need to be overcome in the future. First, chitosan cannot be well dissolved in neutral and alkaline pH. Second, the human toxicity of CS or CS-based NPs needs further investigation. Furthermore, the bactericidal activity of chitosan itself hinders its development, and subsequent modifications should be made to enhance its antibacterial activity and biocompatibility.

### 3. Application of antibacterial chitosan biomaterial in burn

The high water content of hydrogels provides a moist environment for the wound, thus enhancing the cellular immunological response during the healing process. Therefore, the potential of hydrogels in wound healing has received extensive attention. However, a highly hydrated environment of hydrogels is also attractive to pathogenic microorganisms and increases the risk of microbial infection. So endowing hydrogels with antibacterial properties is the primary problem in the development of wound dressing.

Chitosan has been widely used in burn repair due to its excellent biocompatibility, degradability and antibacterial activity (Table 1).<sup>151,164</sup> Ouyang *et al.* developed a new type of dressing by incorporating marine peptides (MPs) into chitosan hydrogels.<sup>165</sup> And it has been shown to be a good restorative effect on burn treatment. Moreover, Bano *et al.* studied the antibacterial and wound healing properties of chitosan-polyvinyl

alcohol combined dressing.<sup>166</sup> The results showed that chitosan had obvious antibacterial effect on pathogenic bacteria. Second degree burns on rabbits showed that chitosan wound dressing could promote the formation of granular and fibrous connective tissue.

#### 3.1 *In situ* injectable chitosan hydrogel

Hydrogels are hydrophilic 3D materials with a large amount of water in their structure, and they have the characteristics of pH-/temperature-/light-responsive and good biocompatibility.<sup>167</sup> The preparation methods of hydrogels are mainly focused on cross-linking, including physical cross-linking (caused by interactions between hydrogen bonds, van der Waals interactions, hydrophobic or electrostatic interactions) or chemical cross-linking (formed by covalent bonds and interactions between various functional groups). Therefore, in the polymerization process, different crosslinking methods can form different polymer structures, such as linear copolymers or graft copolymers.<sup>168</sup> A variety of hydrogels that can respond to external stimuli, including magnetic fields, temperature, light, enzymes, and electric fields, have been studied to meet various practical needs.<sup>169–173</sup>

For example, Qu *et al.* designed a multifunctional injectable hydrogel dressing that combines electrical conductivity, ideal antioxidant capacity, and antibacterial properties to meet the growing need for skin damage.<sup>174</sup> This hydrogel was prepared based on the formation of the Schiff base bond between an oxidized hyaluronic acid-graft-aniline tetramer (OHA-AT) and *N*-carboxyethyl chitosan (CEC). At the same time, the antibiotic amoxicillin was *in situ* encapsulated in the hydrogel to enhance the antibacterial properties of the conductive hydrogel dressing. The chemical structure, electroactivity, conductivity, equalized swelling behavior, rheological properties, cell compatibility, antioxidant capacity, antibacterial activity, and wound healing effect of hydrogels were characterized entirely. The rheological properties of OHA-AT5/CEC hydrogel showed the highest storage modulus of 1400 Pa among all these hydrogels. With the increase of AT, the storage modulus of hydrogel decreases gradually. The degradability of hydrogels was evaluated *in vitro* (PBS at pH 7.4 as a medium). After 9 days of incubation, the OHA-AT5/CEC hydrogel showed a mass loss of 88%, which indicates that the hydrogel formulations had good biodegradable properties and can be used for further *in vivo* application. In addition, the four-point probe method was used to test the conductivity of the hydrogel samples. The hydrogel showed a conductivity of 0.05 mS cm<sup>-1</sup>, with the addition of AT segments in the hydrogels, the conductivity of the hydrogels increased from 0.09 mS cm<sup>-1</sup> to 0.42 mS cm<sup>-1</sup> (within the skin conductivity range: 1 × 10<sup>-4</sup> mS cm<sup>-1</sup> to 2.6 mS cm<sup>-1</sup>). Dressings with skin-like electrical conductivity can facilitate the healing process.<sup>175</sup> The antibacterial properties of the drug-loaded hydrogels were tested by the zone of inhibition (ZOI) experiment. Compared with unloaded hydrogels, amoxicillin encapsulated hydrogels (2 mg amoxicillin per ml hydrogels) showed significant inhibitory zones against *S. aureus* and *E. coli* on the first day, indicating the cumulative diffusion of amoxicillin to the



Table 1 Function and application of different types of antibacterial chitosan hydrogels

Chitosan hydrogels	Hydrogel types	Characters	Functions	Animal model	Ref.
<i>In situ</i> injectable chitosan hydrogels	Silk fibroin hydrogel	<i>In situ</i> forming hydrogel, injectable	SF hydrogel not only promotes wound healing but also shows transitions from inflammation to proliferation stage.	The full-thickness third-degree burn wounds, wistar albino rats.	165
	Methylcellulose (MC) hydrogel	Thermo-responsive, injectable	MC hydrogel with silver oxide NPs exhibited an excellent antimicrobial activity and burn wound healing effect.	Second-degree burns, Sprague-Dawley rats.	45
	Supramolecular host-guest gelatin (HGM) hydrogel	Shear-thinning, injectability	It improved the inflammation of wounds caused by high ROS and oxidative stress, enhanced angiogenesis and accelerated wound healing.	Full-thickness burn wounds, Sprague Dawley rats.	162
	AG-OD-Fe(III) hydrogels	Shape adaptability, injectable, self-healing capability, strong adhesion.	The hydrogel promoted burn wound healing by decreasing the expression of pro-inflammatory cytokines, promoting angiogenesis and promoting collagen deposition.	Deep second-degree models, Kunming mice.	178
Conductive polymeric chitosan material	QCSG/GM/GO hydrogels	Injectable, antimicrobial, conductive.	This hydrogel had good antibacterial property and wound healing ability.	MRSA infected full-thickness skin defect model, Kunming mice.	198
	OHA-AT/CEC hydrogels	Degradable, conductive, anti-oxidant	This hydrogels accelerated wound healing rate with higher granulation tissue thickness, collagen disposition and more angiogenesis.	Full-thickness skin defect model, Kunming mice.	174
	CP/OD hydrogels	Shape memory copolymers with electroactivity, super stretchability and tunable recovery temperature	The electroactive, highly stretchable, biodegradable shape memory polymers with tunable recovery temperature near the body temperature have great potential in skeletal muscle tissue engineering application.		195
Antibacterial phototherapy chitosan hydrogel	Nd-Ca-Si silicate glasses and alginate composite hydrogels	Photothermal property, emit fluorescence, temperature monitoring.	This implantable material with unique temperature monitoring, photothermal function, and wound healing bioactivity can be used for localized thermal therapy.	Second-degree skin burn model, mice BALB/c.	205
	CEC/PF/CNT hydrogel	Conductive, self-healing and adhesive	The conductive photothermal self-healing nanocomposite hydrogels as multifunctional wound dressing exhibit great potential for the treatment of infected wounds.	A mouse full-thickness skin wound-infected model	204
	CSDP-PACT hybrid hydrogel	Portable, light-triggered, anti-bacterial theranostic-platform	The hydrogels augmented wound healing by effective inhibition of bacterial growth, controlled inflammation, higher collagen deposition, and rapid epithelialization	MDR- <i>S. aureus</i> infected burns, Balb/c mice.	206

surroundings which inactivated bacteria in the respective areas. During the *in vivo* wound healing trial, OHA-AT/CEC hydrogels reduced inflammatory infiltration and increased fibroblast density and collagen deposition, as well as granulation tissue thickness.<sup>174</sup>

The injectable hydrogel scaffold can be easily implanted and covered over tissue defects of any shape, as a promising minimally invasive procedure that can reduce patient pain.<sup>176–180</sup> However, infections during or after injecting scaffold remains an inevitable disadvantage, which reduces the therapeutic effectiveness of tissue repair. Therefore, there are still many problems in practical applications to be solved in the future research.

### 3.2 Conductive polymeric chitosan hydrogel

The human body has endogenous bioelectric system. The skin, composed of dermis, epidermis and corneum, is one of the sensitive tissues to electrical signals, and owns conductivity values from  $2.6 \text{ mS cm}^{-1}$  to  $1 \times 10^{-4} \text{ mS cm}^{-1}$ .<sup>175–177</sup> The surface of intact human skin is more negatively charged than deeper skin layers.<sup>178</sup> However, when there is a defect or wound

in the skin, the deeper cells in the epidermis and the cells in the wound are positively charged. The combination of the positively charged wound and negatively charged surrounding intact skin creates an endogenous skin battery. Any damage to its structural integrity leads to a short circuit that generates a current vector at the perimeter of the wound which acts to guide cell migration towards the wound centre, thus directing wound healing.<sup>179</sup> This bioelectric current facilitates wound healing best when the wound tissue is moistened.<sup>180</sup> Many studies have shown that electrical stimulation and electroactivity contribute to good adhesion, proliferation, migration and differentiation of electrical signal-sensitive cells such as nerve, muscle, cardiac, keratinocytes, myoblasts, fibroblasts, cardiomyocytes, osteoblasts and mesenchymal stem cells, *etc.*<sup>181–191</sup> Therefore, the design of new functional wound dressing with electrical conductivity will be more helpful to promote the wound healing process. Currently, studies have been conducted to incorporate conductive polymers into scaffolds and dressings.<sup>192</sup> The increased electrical conductivity of polymers can facilitate therapeutic applications, such as electrical stimulation of wound areas, increase antimicrobial activity,



scavenge free radicals and can control the release of pharmaceutical and biological agents.<sup>193,194</sup>

In addition, smart materials with dual responses have made great progress in tissue repair. Qu *et al.* developed injectable antibacterial conductive hydrogels with dual response to an electric field and pH for localized “smart” drug release.<sup>195</sup> Hydrogels were prepared by mixing a chitosan-graft-polyaniline (CP) copolymer and oxidized dextran (OD). Conductive antimicrobial hydrogels are realized through the inherent antimicrobial properties of chitosan and polyaniline.<sup>196,197</sup> After doping CP with 1 M HCl, a new absorption peak appeared at 435 nm, and  $\pi$ - $\pi^*$  transition of the benzene ring was observed to slightly shift blue to 292 nm. Electroactive materials could be converted to electrical conductors by reversible ion exchange, depending on the transition between the oxidized and reduced states of the material. The conductivity of CP/OD3 hydrogels under swelling conditions was  $6.9 \times 10^{-2} \text{ S m}^{-1}$ , and the conductivity of these hydrogels (CP/OD1, CP/OD3 and CP/OD5) was increased by adding polyaniline to chitosan, which were  $7.6 \times 10^{-2} \text{ S m}^{-1}$ ,  $7.8 \times 10^{-2} \text{ S m}^{-1}$ , and  $7.9 \times 10^{-2} \text{ S m}^{-1}$ , respectively. Electrical response to drug release was performed using an “on-off” pulse release. Amoxicillin/ibuprofen-loaded hydrogel (1.5 mg amoxicillin/ibuprofen loaded in 1 mL CP/OD3 hydrogel) was applied at 3 V for 3 minutes and were repeated after half an hour. In the absence of any voltage, there was a slow release in the first 30 minutes, and a significant increase in the release rate of amoxicillin was observed in the following 3 minutes when 3 V was applied, while the same release behavior was observed in the subsequent cycle. In an *in vitro* model, the pH response behavior was verified by drug release of hydrogels in PBS solutions with different pH values (pH = 7.4 or 5.5). In the initial burst release period, the release rate of amoxicillin in CP/OD1 hydrogel in an acidic environment (pH = 5.5) was significantly faster than that in a physiological environment (pH = 7.4). At pH 5.5, approximately 55% of the drug was released during the initial burst phase after incubation for 45 min, and approximately 99% of the drug was released during 36 h. However, for the hydrogels in PBS at pH 7.4, only 23% of the drug was released after 45 min, and the total cumulative release percentage of the hydrogels was approximately 55% after 36 h. These results indicate that these pH-sensitive hydrogels released significantly more drugs in acidic environments and less drugs in physiological environments, which is important for their practical application as a “smart” pH-sensitive drug carriers.<sup>195</sup>

In another study, Liang *et al.* used GO endowed photothermal properties and conductivity of glycidyl methacrylate functionalized quaternized chitosan/gelatin methacrylate/graphene oxide hydrogels (QCSG/GM/GO). QCSG/GM/GO hydrogels showed a significant temperature increase within 1 min, while the temperature of the hydrogels without GO only fluctuated slightly. In addition, the temperature of QCSG/GM/GO0.5 hydrogel increased only 12 °C, the QCSG/GM/GO1 hydrogel increased by 19 °C, and the QCSG/GM/GO2 hydrogel rose by 23 °C after 10 minutes of NIR irradiation. Therefore, the content of GO can be regulated to achieve the purpose of

antibacterial. On the other hand, the conductivity of QCSG/GM/GO hydrogel increased with the addition of GO. When GO content was 0%, 0.5%, 1% and 2%, the electrical conductivity was  $0.97 \pm 0.052$ ,  $2.29 \pm 0.26$ ,  $4.64 \pm 0.36$  and  $10.07 \pm 2.69 \times 10^{-2} \text{ S m}^{-1}$ , respectively, which made our hydrogel a good candidate material for skin wound dressing.<sup>198</sup>

The various conductive materials mentioned in this review show promising function or potential in wound management or skin tissue engineering, but they have the following limitations for clinical application: (1) biocompatibility and stable expression of conductive materials. (2) Controllability and durability of materials under an electric field. (3) The controlled and delivery of drugs and other bioactive substances. (4) Clinical safety issues. Despite these limitations, conducting polymers merit further scientific research in wound healing and skin tissue engineering.

### 3.3 Antibacterial phototherapy chitosan hydrogel

Antimicrobial phototherapies, such as photothermal and photodynamic therapies, have attracted considerable attention in treating of infected wounds due to their targeted selectivity, non-invasiveness, remote controllability and biological safety.<sup>199–201</sup> When the photothermal wound dressing is irradiated by NIR light, PTT kills microorganisms by raising the local temperature ( $> 50^\circ\text{C}$ ) and causing physical damage (thermal damage) to bacteria.<sup>202</sup> These photothermal materials (including photosensitizer and metal materials) exhibit excellent mechanical, stable photothermal and electronic properties, so they have been extensively studied in tissue engineering research in recent years.<sup>203,204</sup>

Based on CEC and benzaldehyde-terminated Pluronic F127/carbon nanotubes (PF127/CNT), He *et al.* developed a series of conductive self-healing and adhesive nanocomposite hydrogels with significant photothermal antibacterial properties.<sup>204</sup> The addition of CNTs made hydrogels have photothermal antibacterial activity *in vitro/in vivo*. To study the photothermal properties of the CEC/PF/CNT hydrogel, the hydrogel was exposed to a NIR laser for 10 minutes, and the thermal map of the hydrogel was recorded by an infrared thermal camera. The results showed that the infrared thermograph without CNT hydrogels was similar to the surrounding environment. By introducing CNTs, the photothermal response was improved obviously. The  $\Delta T$ s of CEC/PF/CNT1, CEC/PF/CNT2, CEC/PF/CNT3 and CEC/PF/CNT4 increased 16.6, 18.8, 21.1 and 22.6 °C, respectively, indicating that the hydrogels exhibited photothermal behavior by incorporation of CNT. Therefore, the photothermal activity of NIR induced CEC/PF/CNT2 against *E. coli* and *S. aureus* was further tested. The CEC/PF/CNT0 group showed no antibacterial efficiency after 10 min of NIR irradiation. The killing rates of CEC/PF/CNT2 hydrogel against *S. aureus* and *E. coli* were about 45% and 63%, respectively, after 1 min of NIR radiation. When the NIR exposure time was increased to 5 min, more than 80% of the bacteria were killed. In addition, when the irradiation time was extended to 10 min, no bacteria survived and both *S. aureus* and *E. coli* were killed by 100%. Therefore, the hydrogel has an excellent response to NIR stimulation and significant photothermal antimicrobial activity. In another



study, Ma *et al.* reported a multifunctional Nd–Ca–Si silicate glass and glass/alginate composite hydrogel, which not only has photothermal properties, but also emit fluorescence under 808 nm laser irradiation. In particular, its fluorescence intensity is linearly related to the *in situ* temperature. The composite hydrogel can be used in fluorescent temperature measurement, photothermal therapy and burn tissue repair and other applications.<sup>205</sup>

The development of multifunctional biomaterials is of great significance for the treatment of burn infection in the future. Mai *et al.* constructed carboxymethyl chitosan (CMCS)-sodium alginate hybrid hydrogel (CSDP), which was loaded with porphyrin photosensitizer sinoporphyrin sodium (DVDMS) and poly (lactic-co-glycolic acid) (PLGA) coated basic fibroblast growth factor (bFGF) nanospheres, for the treatment of burn by photodynamic antimicrobial chemotherapy (PACT). CSDP hydrogel showed excellent antibacterial and anti-biofilm activities, nearly eradicating 99.99% of *S. aureus* and MDR *S. aureus* (producing ROS to enhance the bactericidal effect) *in vitro*. KEGG analysis revealed that after PACT, multiple signaling pathways of multidrug resistance in MDR *S. aureus* were altered, including the ribosome related pathway, the arginine and peptidoglycan pathway, and the oxidative stress related pathway. In a burn infection model, CSDP-PACT hydrogel effectively inhibited bacteria growth and promoted wound healing. In conclusion, CSDP hydrogel is a light-triggered antibacterial therapy platform. It offers a promising strategy for the treatment of burn infections.<sup>206</sup>

### 3.4 Other polysaccharide-based antibacterial hydrogels

**3.4.1. Gelatin-based antibacterial hydrogels.** Gelatin is a product derived from the hydrolysis of collagen.<sup>207</sup> It is widely used in biomedical field because of its good biocompatibility, biodegradability and non-immunogenicity.<sup>208</sup> In addition, the molecular structure of gelatin contains arginine-glycine-asparagine (RGD) sequence, which can promote cell adhesion, migration and proliferation, making gelatin an ideal tissue repair material.<sup>209</sup> Han *et al.* prepared gelatin-based hydrogels, which had inherent self-healing ability, good cellular compatibility, adhesion, electrical conductivity and excellent hemostatic performance *in vivo*. It has potential application value in tissue adhesives, wound dressings and wearable devices.<sup>209</sup>

Moreover, gelatin-based hydrogels can speed up burn wound repair. Burn wounds are generally accompanied by necrotic tissue, excessive reactive oxygen species and bacterial infection, which further deepens the wound and delays healing.<sup>210</sup> Therefore, the design and development of a multifunctional hydrogel dressing that can both prevent and treat infection and respond to the microenvironment of wound tissues with high reactive oxygen species is an urgent need and challenge. Inspired by mussel chemistry, Han *et al.* constructed an adhesive hydrogel wound dressing with electrical conductivity, antioxidant activity, and photothermal antibacterial activity.<sup>208</sup> The hydrogel showed suitable and adjustable swelling, degradation and rheological properties. In addition, hydrogels had good cytocompatibility and the ability of scavenging intracellular reactive oxygen

species. Finally, *in vivo* data from rat burn models also suggested that hydrogel could accelerate burn wound healing.

**3.4.2. HA-based antibacterial hydrogels.** Hyaluronic acid (HA), is a linear polysaccharide consisting of alternating units of a repeating disaccharide,  $\beta$ -1, 4-D-glucuronic acid- $\beta$ -1, 3-N-acetyl-D-glucosamine, found throughout the body (from the vitreous of the eye to the ECM of cartilage tissues).<sup>211</sup> HA can prevent the proliferation of bacteria, and has antiinflammatory effects, and promotes wound healing.<sup>212</sup>

At present, HA-based injectable hydrogels are mainly constructed by doping antibacterial active molecules (such as chlorhexidine, antimicrobial peptides, antibiotics, metal ions, *etc.*).<sup>213–215</sup> For example, in 2019, Dong *et al.* prepared a series of adhesive hemostatic antioxidant conductive photothermal antibacterial hydrogels based on HA grafted dopamine and reduced graphene oxide (rGO) for wound dressings using H<sub>2</sub>O<sub>2</sub>/HPR (horseradish peroxidase) systems.<sup>216</sup> These hydrogels exhibit high swelling, degradability, adjustable rheological property, and similar or superior mechanical properties to human skin. Moreover, the polydopamine endowed hydrogels with antioxidant activity, conductivity, and NIR irradiation enhanced *in vivo* antibacterial behavior. Furthermore, the hydrogel dressings significantly enhanced vascularization by upregulating growth factor expression of CD31 and improved the granulation tissue thickness and collagen deposition.

### 3.5 Application of polysaccharide-based hydrogels in clinical

Burn wounds are susceptible to infection by pathogenic bacteria (such as *E. coli*, *S. aureus*, *P. aeruginosa*, *S. epidermidis* and *fungal communities*), thus prolonging wound healing time. The control of bacterial infection has always been the focus of the wound dressing and tissue repair process to reduce the likelihood of wound infection. Nano silver, antibiotics, antimicrobial peptides, *etc.* have been routinely used in clinical/preclinical bacterial infections. For example, Oryan *et al.* topical application of chitosan-capped silver nanoparticles (Ch/AgNPs) to treat burns.<sup>217</sup> Ch/AgNPs significantly hasten the healing process by reducing the inflammatory cells, increasing proliferation, migrations, and proliferation of fibroblasts and promoting granulation tissue maturation.<sup>217</sup> In conclusion, polysaccharide-based hydrogels are the most common clinical/preclinical strategy for reducing the incidence of burn wound infection by controlling bacterial infection.

At present, a variety of commercial wound dressings have been developed, ranging from natural polymers to various other forms of synthetic polymers. The emergence of antibiotic resistance has forced researchers to seek novel polysaccharide hydrogel wound dressings with antimicrobial activity. Among them, natural polysaccharides represented by chitosan are famous for their excellent bactericidal and hemostatic properties. Based on the excellent properties of chitosan, a variety of wound dressings are already on the market, namely Axiostat<sup>®</sup>, Tegaserb<sup>®</sup> and KytoCel<sup>®</sup>.<sup>218</sup> Of these, Axiostat<sup>®</sup> can control bleeding. Tegaserb<sup>®</sup> can treat a wide range of internal injuries. KytoCel<sup>®</sup> combines with wound exudate to form a clear gel that absorbs pathogens and is hemostatic.



However, there are still limitations in the development of polysaccharide hydrogels. It has low mechanical properties. Modify the structure of polysaccharides. Hydrogels usually need to be doped with silver ( $\text{Ag}^+$ ), iron ( $\text{Fe}^{3+}$ ), strontium ( $\text{Sr}^{2+}$ ), zinc ( $\text{Zn}^{2+}$ ) and other metallic ions. Toxicity needs to be further verified. Few injectable polysaccharide hydrogels are available for clinical transformation, especially in the field of regenerative medicine.

## 4. Conclusions

Burn is a complex injury, especially large area burns and elderly burns have a relatively high mortality rate.<sup>219</sup> Burns with large wounds, irregular and severe hemorrhage are more likely to cause infections and slow healing than other injuries.<sup>220</sup> Therefore, prevention and treatment of burn infection have become a critical link in healing.

Over the past few decades, some efforts have been made to improve the treatment of burn infections. In recent years, technological developments in nanomedicine have contributed to the search for new alternatives to overcome bacterial infections. Several types of nanoparticles, such as metal nanoparticles, nano-micelles, and polymer nanoparticles, have been proposed to enhance the antimicrobial activity of compounds. Hence, in this review, we focus on both organic and non-organic nanoparticles, including metal/metal oxides nanoparticles ( $\text{AgNPs}$ ,  $\text{AuNPs}$ ,  $\text{CuNPs}$ ,  $\text{ZnO}$ , and  $\text{TiO}_2$ ) and polymeric nanoparticles (chitosan and polymer micelles), all of which could be possibly utilized as potential antimicrobial agents in burns. We believe that the development of simple, low-cost nanoparticles antimicrobials may be the future direction of pharmaceuticals and medicine.

In recent years, multifunctional biocompatible hydrogel scaffolds have been developed rapidly, such as wound dressings and films, stimulation-responsive hydrogels and hydrogels for delivering bioactive substances. Up to now, hydrogels for the treatment of burns include the following aspects: designing hydrogels with good biocompatibility and biodegradability, intelligent hydrogel systems (light response, pH-response and temperature response) were designed based on synthesis techniques (such as photo-crosslinking and dynamic physical chemistry crosslinking) to achieve controlled release of antibacterial materials. To investigate the affinity of hydrogel materials to damaged tissues, such as cell adhesion, migration and proliferation in hydrogel.

There are still many problems to be solved in the future research. Firstly, the lack of clinical animal models. At present, most experimental animal models are healthy young animals, and there is little discussion on some old animals or animal models with diseases. In addition, hydrogels are easily damaged during transportation and storage, which will eventually lead to drug leakage and affect their structure and function. Furthermore, the degradation rate of hydrogels should match the regeneration speed of the wound. Finally, appropriate hydrogels should be given for different tissue wounds. Therefore, an inexpensive, easy to manufacture, preserve, and suitable for all types of people

should be developed in the future to provide a promising future for the treatment of burn infection.

## Abbreviations

PDGF	Platelet-derived growth factor
EGF	Epidermal growth factor
TGF- $\beta$	Transforming growth factor- $\beta$
TNF- $\alpha$	Tumor necrosis factor
IL-1	Interleukin-1
IL-6	Interleukin-1
IL-8	Interleukin-8
VEGF	Vascular endothelial growth factor
FGF	Fibroblast growth factor
IGF-1	Insulin-like growth factor
NGF	Nerve growth factor
KGF	Keratinocyte growth factor
bFGF	Basic fibroblast growth factor
ECM	Extracellular matrix
GM-CSF	Granulocyte-macrophage colony stimulating factor
MMPs	Matrix metalloproteinases
TIMPs	Tissue inhibitors of metalloproteinases
MDR	Multidrug-resistant
7-ADCA	7-Aminodesacetoxycephalosporanic acid
APA	6-Aminopenicillanic acid
ROS	Reactive oxygen species
GDY	Graphdiyne
BC	Bacterial cellulose
TC	Tetracycline
CC	Citric modified chitosan
MC	Minocycline
PVA	Polyvinyl alcohol
HNT	Halloysite nanotubes
SF	Silk fibroin
FA	Fusidic acid
AMPs	Antimicrobial peptides
LTF	Lactotransferrin
HPC	Hydroxypropyl cellulose
MRSA	Methicillin-resistant <i>Staphylococcus aureus</i>
AgSD	Silver sulfadiazine
TCTS	Temperature-sensitive chitosan
DD	Deacetylation
OHA-AT	Oxidized hyaluronic acid-graft-aniline tetramer
CEC	N-Carboxyethyl chitosan
ZOI	Zone of inhibition
OD	Oxidized dextran
CP	Chitosan-graft-polyaniline
QCSG/GM/GO	Quaternized chitosan/gelatin methacrylate/graphene oxide hydrogels

## Author contributions

Que Bai: funding acquisition, methodology, and writing – original draft. Caiyun Zheng: resources, conceptualization,



and validation. Wenting Chen: investigation and data curation. Na Sun: project administration and validation. Qian Gao: formal analysis and software. Jinxi Liu: data curation, methodology, and visualization. Fangfang Hu: validation and project administration. SaHu Pimpri: data curation and formal analysis. Xintao Yan: data curation and methodology. Yanni Zhang: supervision and funding acquisition. Tingli Lu: conceptualization, funding acquisition, writing – review & editing.

## Conflicts of interest

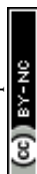
The authors declare no conflict of interest.

## Acknowledgements

We acknowledge funding support by the joint funding from Department of Science and Technology of Shaanxi Province and Northwestern Polytechnical University (No. 2020GXLH-Z-021) and the innovation foundation for doctor dissertation of Northwestern Polytechnical University (No. CX2021099).

## References

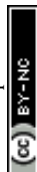
- 1 R. Norton and O. Kobusingye, *N. Engl. J. Med.*, 2013, **368**, 1723–1730.
- 2 D. G. Greenhalgh, *N. Engl. J. Med.*, 2019, **380**, 2349–2359.
- 3 M. A. Mofazzal Jahromi, P. Sahandi Zangabad, S. M. Moosavi Basri, K. Sahandi Zangabad, A. Ghamarypour, A. R. Aref, M. Karimi and M. R. Hamblin, *Adv. Drug Delivery Rev.*, 2018, **123**, 33–64.
- 4 M. G. Jeschke, M. E. van Baar, M. A. Choudhry, K. K. Chung, N. S. Gibran and S. Logsetty, *Nat. Rev. Dis. Primers.*, 2020, **6**, 11.
- 5 S. Hettiaratchy and P. Dziewulski, *BMJ*, 2004, **328**, 1427–1429.
- 6 H. K. Akelma and Z. A. Karahan, Rare chemical burns: Review of the literature, *Int Wound J.*, 2019, **16**, 1330–1338.
- 7 S. A. Wells, *Curr. Probl. Surg.*, 1997, **34**, 681.
- 8 M. Madaghiele, C. Demitri, A. Sannino and L. Ambrosio, Polymeric hydrogels for burn wound care: Advanced skin wound dressings and regenerative templates, *Burns Trauma*, 2014, **2**(4), 2321–3868.
- 9 M. P. Rowan, L. C. Cancio, E. A. Elster, D. M. Burmeister, L. F. Rose, S. Natesan, R. K. Chan, R. J. Christy and K. K. Chung, *Crit. Care*, 2015, **19**, 12.
- 10 L. Li and M. Xiao, Role of Autophagy in Burn Wound Progression and Wound Healing, 2016.
- 11 L. Rittie, *J. Cell Commun. Signaling*, 2016, **10**, 103–120.
- 12 S. W. Geoffrey, C. Gurtner, Y. Barrandon and M. T. Longaker, Wound repair and regeneration, *Nature*, 2008, **453**, 314–321.
- 13 N. Strbo, N. Yin and O. Stojadinovic, *Adv. Wound Care*, 2014, **3**, 492–501.
- 14 J. Li, J. Chen and R. Kirsner, *Clin. Dermatol*, 2007, **25**, 9–18.
- 15 I. Pastar, O. Stojadinovic, N. C. Yin, H. Ramirez, A. G. Nusbaum, A. Sawaya, S. B. Patel, L. Khalid, R. R. Isseroff and M. Tomic-Canic, *Adv. Wound Care*, 2014, **3**, 445–464.
- 16 P. Martin and D. B. Gurevich, *Semin. Cell Dev. Biol.*, 2021, **119**, 101–110.
- 17 T. S. Leyane, S. W. Jere and N. N. Houreld, *Int. J. Mol. Sci.*, 2021, 22.
- 18 T. N. Demidova-Rice, M. R. Hamblin and I. M. Herman, *Adv. Skin Wound Care*, 2012, **25**, 349–370.
- 19 B. Hinz, *J. Invest. Dermatol.*, 2007, **127**, 526–537.
- 20 Y. K. Coban, *World J. Crit. Care Med.*, 2012, **1**, 94–101.
- 21 W. Norbury, D. N. Herndon, J. Tanksley, M. G. Jeschke, C. C. Finnerty and I Sci Study Comm Surgical, *Surg. Infect.*, 2016, **17**, 250–255.
- 22 J. W. Shupp, A. R. Pavlovich, J. C. Jeng, J. C. Pezzullo, W. J. Oetgen, A. D. Jaskille, M. H. Jordan and S. Shoham, *J. Burn Care Res.*, 2010, **31**, 521–528.
- 23 R. Cartotto, *Int. J. Burns Trauma*, 2017, **5**, 33.
- 24 M. Sevgi, A. Toklu, D. Vecchio and M. R. Hamblin, *Recent Pat. Anti-Infect. Drug Discovery*, 2013, **8**, 161–197.
- 25 J. Qu, X. Zhao, Y. P. Liang, T. L. Zhang, P. X. Ma and B. L. Guo, *Biomaterials*, 2018, **183**, 185–199.
- 26 S. Q. Li, S. J. Dong, W. G. Xu, S. C. Tu, L. S. Yan, C. W. Zhao, J. X. Ding and X. S. Chen, *Adv. Sci.*, 2018, **5**, 17.
- 27 T. R. Kyriakides, A. Raj, T. H. Tseng, H. Xiao, R. Nguyen, F. S. Mohammed, S. Halder, M. Q. Xu, M. J. Wu, S. Z. Bao and W. C. Sheu, *Biomed. Mater.*, 2021, **16**, 26.
- 28 Y. H. Zheng, Y. L. Cheng, J. J. Chen, J. X. Ding, M. Q. Li, C. Li, J. C. Wang and X. S. Chen, *ACS Appl. Mater. Interfaces*, 2017, **9**, 3487–3496.
- 29 L. Y. Wei, J. J. Chen, S. H. Zhao, J. X. Ding and X. S. Chen, *Acta Biomater.*, 2017, **58**, 44–53.
- 30 S. Koutsopoulos, *Adv. Drug Delivery Rev.*, 2012, **64**, 1459–1476.
- 31 M. Moritz and M. Geszke-Moritz, *Chem. Eng. J.*, 2013, **228**, 596–613.
- 32 M. Rai, A. Yadav and A. Gade, *Biotechnol. Adv.*, 2009, **27**, 76–83.
- 33 A. Heyneman, H. Hoeksema, D. Vandekerckhove, A. Pirayesh and S. Monstrey, *Burns*, 2016, **42**, 1377–1386.
- 34 M. Mirafteb, R. Masood and V. Edward-Jones, *Carbohydr. Polym.*, 2014, **101**, 1184–1190.
- 35 Z. J. Fan, B. Liu, J. Q. Wang, S. Y. Zhang, Q. Q. Lin, P. W. Gong, L. M. Ma and S. R. Yang, *Adv. Funct. Mater.*, 2014, **24**, 3933–3943.
- 36 J. S. Mohler, W. Sim, M. A. T. Blaskovich, M. A. Cooper and Z. M. Ziora, *Biotechnol. Adv.*, 2018, **36**, 1391–1411.
- 37 A. C. Burdusel, O. Gherasim, A. M. Grumezescu, L. Mogoanta, A. Fica and E. Andronescu, *Nanomaterials*, 2018, **8**, 25.
- 38 C. Y. Chen, H. Yin, X. Chen, T. H. Chen, H. M. Liu, S. S. Rao, Y. J. Tan, Y. X. Qian, Y. W. Liu, X. K. Hu, M. J. Luo, Z. X. Wang, Z. Z. Liu, J. Cao, Z. H. He, B. Wu, T. Yue, Y. Y. Wang, K. Xia, Z. W. Luo, Y. Wang, W. Y. Situ, W. E. Liu, S. Y. Tang and H. Xie, *Sci. Adv.*, 2020, **6**, 14.
- 39 V. Gopinath, S. Priyadarshini, M. F. Loke, J. Arunkumar, E. Marsili, D. MubarakAli, P. Velusamy and J. Vadivelu, *Arabian J. Chem.*, 2017, **10**, 1107–1117.



- 40 S. Batool, Z. Hussain, M. B. K. Niazi, U. Liaqat and M. Afzal, *J. Drug Delivery Sci. Technol.*, 2019, **52**, 403–414.
- 41 M. Yadollahi, H. Namazi and M. Aghazadeh, *Int. J. Biol. Macromol.*, 2015, **79**, 269–277.
- 42 M. H. Kim, H. Park, H. C. Nam, S. R. Park, J. Y. Jung and W. H. Park, *Carbohydr. Polym.*, 2018, **181**, 579–586.
- 43 Y. Z. Zhou, R. Chen, T. T. He, K. Xu, D. Du, N. Zhao, X. N. Cheng, J. Yang, H. F. Shi and Y. H. Lin, *ACS Appl. Mater. Interfaces*, 2016, **8**, 15067–15075.
- 44 S. Jiji, S. Udhayakumar, K. Maharajan, C. Rose, C. Muralidharan and K. Kadirvelu, *Carbohydr. Polym.*, 2020, **245**, 11.
- 45 C. Kalirajan and T. Palanisamy, *Adv. Healthcare Mater.*, 2020, **9**, 15.
- 46 L. J. V. Piddock, *Nat. Rev. Microbiol.*, 2017, **15**, 639–640.
- 47 A. Panacek, L. Kvitek, M. Smekalova, R. Vecerova, M. Kolar, M. Roderova, F. Dycka, M. Sebel, R. Prucek, O. Tomanec and R. Zboril, *Nat. Nanotechnol.*, 2018, **13**, 65–71.
- 48 L. D. Kong, C. S. Alves, W. X. Hou, J. R. Qiu, H. Mohwald, H. Tomas and X. Y. Shi, *ACS Appl. Mater. Interfaces*, 2015, **7**, 4833–4843.
- 49 S. Wang, C. Yan, X. M. Zhang, D. Z. Shi, L. X. Chi, G. X. Luo and J. Deng, *Biomater. Sci.*, 2018, **6**, 2757–2772.
- 50 P. C. L. Silveira, M. Venancio, P. S. Souza, E. G. Victor, F. d S. Notoya, C. S. Paganini, E. L. Streck, L. da Silva, R. A. Pinho and M. M. S. Paula, *Mater. Sci. Eng., C*, 2014, **44**, 380–385.
- 51 S. C. Wei, L. Chang, C. C. Huang and H. T. Chang, *Biomater. Sci.*, 2019, **7**, 4482–4490.
- 52 Y. Cui, Y. Y. Zhao, Y. Tian, W. Zhang, X. Y. Lu and X. Y. Jiang, *Biomaterials*, 2012, **33**, 2327–2333.
- 53 X. L. Yang, J. C. Yang, L. Wang, B. Ran, Y. X. Jia, L. M. Zhang, G. Yang, H. W. Shao and X. Y. Jiang, *ACS Nano*, 2017, **11**, 5737–5745.
- 54 Y. Qiao, J. He, W. Y. Chen, Y. H. Yu, W. L. Li, Z. Du, T. T. Xie, Y. Ye, S. Y. Hua, D. N. Zhong, K. Yao and M. Zhou, *ACS Nano*, 2020, **14**, 3299–3315.
- 55 N. Jones, B. Ray, K. T. Ranjit and A. C. Manna, *FEMS Microbiol. Lett.*, 2008, **279**, 71–76.
- 56 Q. Shi, X. Luo, Z. Huang, A. C. Midgley, B. Wang, R. Liu, D. Zhi, T. Wei, X. Zhou, M. Qiao, J. Zhang, D. Kong and K. Wang, *Acta Biomater.*, 2019, **86**, 465–479.
- 57 L. Kong, Z. Wu, H. Zhao, H. Cui, J. Shen, J. Chang, H. Li and Y. He, *ACS Appl. Mater. Interfaces*, 2018, **10**, 30103–30114.
- 58 A. Nasajpour, S. Ansari, C. Rinoldi, A. S. Rad, T. Aghaloo, S. R. Shin, Y. K. Mishra, R. Adelung, W. Swieszkowski, N. Annabi, A. Khademhosseini, A. Moshaverinia and A. Tamayol, *Adv. Funct. Mater.*, 2018, **28**, 8.
- 59 Y. Yang, L. Ma, C. Cheng, Y. Y. Deng, J. B. Huang, X. Fan, C. X. Nie, W. F. Zhao and C. D. Zhao, *Adv. Funct. Mater.*, 2018, **28**, 12.
- 60 J. B. You, L. Meng, T. B. Song, T. F. Guo, Y. Yang, W. H. Chang, Z. R. Hong, H. J. Chen, H. P. Zhou, Q. Chen, Y. S. Liu, N. De Marco and Y. Yang, *Nat. Nanotechnol.*, 2016, **11**, 75–81.
- 61 M. J. Choi, S. Kim, H. Lim, J. Choi, D. M. Sim, S. Yim, B. T. Ahn, J. Y. Kim and Y. S. Jung, *Adv. Mater.*, 2016, **28**, 1780–1787.
- 62 S. Noimark, J. Weiner, N. Noor, E. Allan, C. K. Williams, M. S. P. Shaffer and I. P. Parkin, *Adv. Funct. Mater.*, 2015, **25**, 1367–1373.
- 63 Y. Li, W. Zhang, J. F. Niu and Y. S. Chen, *ACS Nano*, 2012, **6**, 5164–5173.
- 64 Z. Hadisi, M. Farokhi, H. R. Bakhsheshi-Rad, M. Jahanshahi, S. Hasanpour, E. Pagan, A. Dolatshahi-Pirouz, Y. S. Zhang, S. C. Kundu and M. Akbari, *Macromol. Biosci.*, 2020, **20**, 17.
- 65 W. J. Miao, H. J. Kim, V. Gujrati, J. Y. Kim, H. Jon, Y. Lee, M. Choi, J. Kim, S. Lee, D. Y. Lee, S. Kang and S. Jon, *Theranostics*, 2016, **6**, 2367–2379.
- 66 Y. T. Kang, X. Y. Tang, Z. G. Cai and X. Zhang, *Adv. Funct. Mater.*, 2016, **26**, 8920–8931.
- 67 F. L. Gao, M. Z. Sun, W. Ma, X. L. Wu, L. Q. Liu, H. Kuang and C. L. Xu, *Adv. Mater.*, 2017, **29**, 8.
- 68 N. Ninan, A. Forget, V. P. Shastri, N. H. Voelcker and A. Blencowe, *ACS Appl. Mater. Interfaces*, 2016, **8**, 28511–28521.
- 69 S. H. Bhang, W. S. Jang, J. Han, J. K. Yoon, W. G. La, E. Lee, Y. S. Kim, J. Y. Shin, T. J. Lee, H. K. Baik and B. S. Kim, *Adv. Funct. Mater.*, 2017, **27**, 13.
- 70 C. Y. Mao, Y. M. Xiang, X. M. Liu, Z. D. Cui, X. J. Yang, K. W. K. Yeung, H. B. Pan, X. B. Wang, P. K. Chu and S. L. Wu, *ACS Nano*, 2017, **11**, 9010–9021.
- 71 P. Wang, L. Jiang and R. X. Han, *Mater. Res. Express*, 2020, **7**, 9.
- 72 A. V. Thanusha, A. K. Dinda and V. Koul, *Mater. Sci. Eng., C*, 2018, **89**, 378–386.
- 73 D. D. Li, Q. Q. Guo, L. M. Ding, W. Zhang, L. Cheng, Y. Q. Wang, Z. B. Xu, H. H. Wang and L. Z. Gao, *ChemBioChem*, 2020, **21**, 2620–2627.
- 74 K. S. Brammer, C. J. Frandsen and S. Jin, *Trends Biotechnol.*, 2012, **30**, 315–322.
- 75 J. Liu, L. J. Ye, Y. L. Sun, M. H. Hu, F. Chen, S. Wegner, V. Mailander, W. Steffen, M. Kappl and H. J. Butt, *Adv. Mater.*, 2020, **32**, 8.
- 76 N. A. Ismail, K. A. M. Amin, F. A. A. Majid and M. H. Razali, *Mater. Sci. Eng., C*, 2019, **103**, 9.
- 77 R. Wang, M. S. Shi, F. Y. Xu, Y. Qiu, P. Zhang, K. L. Shen, Q. Zhao, J. G. Yu and Y. F. Zhang, *Nat. Commun.*, 2020, **11**, 12.
- 78 M. Li, Z. Ma, Y. Zhu, H. Xia, M. Y. Yao, X. Chu, X. L. Wang, K. Yang, M. Y. Yang, Y. Zhang and C. B. Mao, *Adv. Healthcare Mater.*, 2016, **5**, 557–566.
- 79 Z. J. Jia, P. Xiu, M. Li, X. C. Xu, Y. Y. Shi, Y. Cheng, S. C. Wei, Y. F. Zheng, T. F. Xi, H. Cai and Z. J. Liu, *Biomaterials*, 2016, **75**, 203–222.
- 80 A. Khalid, H. Ullah, M. Ul-Islam, R. Khan, S. Khan, F. Ahmad, T. Khan and F. Wahid, *RSC Adv.*, 2017, **7**, 47662–47668.
- 81 G. A. Seisenbaeva, K. Fromell, V. V. Vinogradov, A. N. Terekhov, A. V. Pakhomov, B. Nilsson, K. N. Ekdahl, V. V. Vinogradov and V. G. Kessler, *Sci. Rep.*, 2017, **7**, 11.



- 82 S. Khan, M. Ul-Islam, W. A. Khattak, M. W. Ullah and J. K. Park, *Cellulose*, 2015, **22**, 565–579.
- 83 C. C. Zhang, Y. D. Li, Y. J. Hu, Y. Peng, Z. Ahmad, J. S. Li and M. W. Chang, *ACS Appl. Mater. Interfaces*, 2019, **11**, 7823–7835.
- 84 X. Y. Li, Q. J. He and J. L. Shi, *ACS Nano*, 2014, **8**, 1309–1320.
- 85 S. B. Hartono, W. Y. Gu, F. Kleitz, J. Liu, L. Z. He, A. P. J. Middelberg, C. Z. Yu, G. Q. Lu and S. Z. Qiao, *ACS Nano*, 2012, **6**, 2104–2117.
- 86 S. Quignard, T. Coradin, J. J. Powell and R. Jugdaohsingh, *Colloids Surf., B*, 2017, **155**, 530–537.
- 87 M. Mehrasa, M. A. Asadollahi, B. Nasri-Nasrabadi, K. Ghaedi, H. Salehi, A. Dolatshahi-Pirouz and A. Arpanaei, *Mater. Sci. Eng., C*, 2016, **66**, 25–32.
- 88 C. Kalirajan and T. Palanisamy, *Biomater. Sci.*, 2020, **8**, 1622–1637.
- 89 P. Appelgren, V. Bjornhagen, K. Bragderyd, C. E. Jonsson and U. Ransjo, *Burns*, 2002, **28**, 39–46.
- 90 A. Saito, H. Miyazaki, T. Fujie, S. Ohtsubo, M. Kinoshita, D. Saitoh and S. Takeoka, *Acta Biomater.*, 2012, **8**, 2932–2940.
- 91 J. M. Chen, Z. G. Liu, M. H. Chen, H. Zhang and X. H. Li, *Macromol. Biosci.*, 2016, **16**, 1368–1380.
- 92 S. Kalita, B. Devi, R. Kandimalla, K. K. Sharma, A. Sharma, K. Kalita, A. C. Katakai and J. Kotoky, *Int. J. Nanomed.*, 2015, **10**, 2971–2984.
- 93 S. Kalita, R. Kandimalla, B. Devi, B. Kalita, K. Kalita, M. Deka, A. C. Katakai, A. Sharma and J. Kotoky, *RSC Adv.*, 2017, **7**, 1749–1758.
- 94 A. Shah, M. A. Buabeid, E. S. A. Arafa, I. Hussain, L. H. Li and G. Murtaza, *Int. J. Pharm.*, 2019, **564**, 22–38.
- 95 A. C. Alavarase, F. W. D. Silva, J. T. Colque, V. M. da Silva, T. Prieto, E. C. Venancio and J. J. Bonvent, *Mater. Sci. Eng., C*, 2017, **77**, 271–281.
- 96 T. Fujie, A. Saito, M. Kinoshita, H. Miyazaki, S. Ohtsubo, D. Saitoh and S. Takeoka, *Biomaterials*, 2010, **31**, 6269–6278.
- 97 H. Chen, B. Y. Li, B. Feng, H. Wang, H. H. Yuan and Z. W. Xu, *RSC Adv.*, 2019, **9**, 19523–19530.
- 98 N. Garrido-Mesa, A. Zarzuelo and J. Galvez, *Br. J. Pharmacol.*, 2013, **169**, 337–352.
- 99 S. Chopra, K. Harjai and S. Chhibber, *Int. J. Med. Microbiol.*, 2016, **306**, 707–716.
- 100 K. Guney, S. Tatar, B. Ozel, C. Seymen, C. Elmas, S. Tuncer and S. Cenetoglu, *Facial Plast. Surg.*, 2019, **35**, 96–102.
- 101 A. Mohebbali, M. Abdouss and F. A. Taromi, *Mater. Sci. Eng., C*, 2020, **110**, 10.
- 102 S. K. Bajpai, V. Pathak and B. Soni, *Int. J. Biol. Macromol.*, 2015, **79**, 76–85.
- 103 A. Mohebbali and M. Abdouss, *Int. J. Biol. Macromol.*, 2020, **164**, 4193–4204.
- 104 P. Kaur, V. S. Gondil and S. Chhibber, *Int. J. Pharm.*, 2019, **572**, 13.
- 105 H. Asgarirad, P. Ebrahimnejad, M. A. Mahjoub, M. Jalalian, H. Morad, R. Ataei, S. S. Hosseini and A. Farmoudeh, *J. Microencapsulation*, 2021, **38**, 100–107.
- 106 Y. Lan, W. C. Li, R. Guo, Y. Zhang, W. Xue and Y. M. Zhang, *J. Biomater. Sci., Polym. Ed.*, 2014, **25**, 75–87.
- 107 Y. Lan, W. C. Li, Y. P. Jiao, R. Guo, Y. Zhang, W. Xue and Y. M. Zhang, *Acta Biomater.*, 2014, **10**, 3167–3176.
- 108 M. Zilberman, D. Egozi, M. Shemesh, A. Keren, E. Mazor, M. Baranes-Zeevi, N. Goldstein, I. Berdicevsky, A. Gilhar and Y. Ullmann, *Acta Biomater.*, 2015, **22**, 155–163.
- 109 A. Gonzalez-Ruiz, R. A. Seaton and K. Hamed, *Infect. Drug Resist.*, 2016, **9**, 47–58.
- 110 L. Robbel and M. A. Marahiel, *J. Biol. Chem.*, 2010, **285**, 27501–27508.
- 111 O. Simonetti, G. Lucarini, F. Orlando, E. Pierpaoli, R. Ghiselli, M. Provinciali, P. Castelli, M. Guerrieri, R. Di Primio, A. Offidani, A. Giacometti and O. Cirioni, *Antimicrob. Agents Chemother.*, 2017, **61**, 11.
- 112 S. Wadhwa, B. Singh, G. Sharma, K. Raza and O. P. Katare, *Drug Delivery*, 2016, **23**, 1204–1213.
- 113 K. Thakur, G. Sharma, B. Singh, S. Chhibber and O. P. Katare, *Drug Delivery Transl. Res.*, 2019, **9**, 748–763.
- 114 B. H. Hu, C. Owh, P. L. Chee, W. R. Leow, X. Liu, Y. L. Wu, P. Z. Guo, X. J. Loh and X. D. Chen, *Chem. Soc. Rev.*, 2018, **47**, 14.
- 115 E. R. Angert, *Nat. Rev. Microbiol.*, 2005, **3**, 214–224.
- 116 C. A. Michael, D. Dominey-Howes and M. Labbate, *Front. Public Health*, 2014, **2**, 145.
- 117 M. Xiong, M. Chen and J. Zhang, *Chem. Biol. Drug Des.*, 2016, **88**, 404–410.
- 118 M. L. Mangoni, A. M. McDermott and M. Zasloff, *Exp. Dermatol.*, 2016, **25**, 167–173.
- 119 L. Otvos, Jr., *Acta Microbiol. Immunol. Hung.*, 2016, **63**, 257–277.
- 120 N. Raheem and S. K. Straus, *Front. Microbiol.*, 2019, **10**, 14.
- 121 G. Zhong, J. Cheng, Z. C. Liang, L. Xu, W. Lou, C. Bao, Z. Y. Ong, H. Dong, Y. Y. Yang and W. Fan, *Adv. Healthcare Mater.*, 2017, **6**.
- 122 C. Bjorn, L. Noppa, E. N. Salomonsson, A.-L. Johansson, E. Nilsson, M. Mahlapuu and J. Hakansson, *Int. J. Antimicrob. Agents*, 2015, **45**, 519–524.
- 123 J. V. Carratala, N. Serna, A. Villaverde, E. Vazquez and N. Ferrer-Miralles, *Biotechnol. Adv.*, 2020, **44**, 13.
- 124 P. Pomastowski, M. Sprynskyy, P. Zuvela, K. Rafinska, M. Milanowski, J. J. Liu, M. G. Yi and B. Buszewski, *J. Am. Chem. Soc.*, 2016, **138**, 7899–7909.
- 125 C. Ghosh, G. B. Manjunath, M. M. Konai, D. S. S. M. Uppu, K. Paramanandham, B. R. Shome, R. Ravikumar and J. Halder, *ACS Infect. Dis.*, 2016, **2**, 111–122.
- 126 M. Pan, C. Lu, M. C. Zheng, W. Zhou, F. L. Song, W. D. Chen, F. Yao, D. J. Liu and J. F. Cai, *Adv. Healthcare Mater.*, 2020, **9**, 12.
- 127 Z. Ozkurt, M. Ertek, S. Erol, U. Altoparlak and M. N. Akcay, *Burns*, 2005, **31**, 870–873.
- 128 E. E. Tredget, H. A. Shankowsky, R. Rennie, R. E. Burrell and S. Logsetty, *Burns*, 2004, **30**, 3–26.
- 129 E. Myhrman, J. Hakansson, K. Lindgren, C. Bjorn, V. Sjostrand and M. Mahlapuu, *Appl. Microbiol. Biotechnol.*, 2013, **97**, 3085–3096.



- 130 J. Hakansson, C. Bjorn, K. Lindgren, E. Sjostrom, V. Sjostrand and M. Mahlapuu, *Antimicrob. Agents Chemother.*, 2014, **58**, 2982–2984.
- 131 S. Y. C. Tong, J. S. Davis, E. Eichenberger, T. L. Holland and V. G. Fowler, *Clin. Microbiol. Rev.*, 2015, **28**, 603–661.
- 132 S. Lakhundi and K. Y. Zhang, *Clin. Microbiol. Rev.*, 2018, **31**, 103.
- 133 E. M. Haisma, A. de Breij, H. Chan, J. T. van Dissel, J. W. Drijfhout, P. S. Hiemstra, A. El Ghalbzouri and P. H. Nibbering, *Antimicrob. Agents Chemother.*, 2014, **58**, 4411–4419.
- 134 Z. Ma, J. Han, B. Chang, L. Gao, Z. Lu, F. Lu, H. Zhao, C. Zhang and X. Bie, *ACS Infect. Dis.*, 2017, **3**, 820–832.
- 135 R. T. Rozenbaum, L. Z. Su, A. Umerska, M. Eveillard, J. Hakansson, M. Mahlapuu, F. Huang, J. F. Liu, Z. K. Zhang, L. Q. Shi, H. C. van der Mei, H. J. Busscher and P. K. Sharma, *J. Controlled Release*, 2019, **293**, 73–83.
- 136 S. Obuobi, H. K. L. Tay, N. D. T. Tram, V. Selvarajan, J. S. Khara, Y. Wang and P. L. R. Ee, *J. Controlled Release*, 2019, **313**, 120–130.
- 137 M. D. Seo, H. S. Won, J. H. Kim, T. Mishig-Ochir and B. J. Lee, *Molecules*, 2012, **17**, 12276–12286.
- 138 A. L. Lakes, R. Peyyala, J. L. Ebersole, D. A. Puleo, J. Z. Hilt and T. D. Dziubla, *Biomacromolecules*, 2014, **15**, 3009–3018.
- 139 J. Reinbold, A. K. Uhde, I. Muller, T. Weindl, J. Geis-Gerstorfer, C. Schlensak, H. P. Wendel and S. Krajewski, *Molecules*, 2017, **22**, 15.
- 140 R. T. C. Cleophas, J. Sjollem, H. J. Busscher, J. A. W. Kruijtzter and R. M. J. Liskamp, *Biomacromolecules*, 2014, **15**, 3390–3395.
- 141 B. S. Atiyeh, M. Costagliola, S. N. Hayek and S. A. Dibo, *Burns*, 2007, **33**, 139–148.
- 142 K. Ito, A. Saito, T. Fujie, K. Nishiwaki, H. Miyazaki, M. Kinoshita, D. Saitoh, S. Ohtsubo and S. Takeoka, *Acta Biomater.*, 2015, **24**, 87–95.
- 143 P. M. Kumar and A. Ghosh, *Eur. J. Pharm. Sci.*, 2017, **96**, 243–254.
- 144 K. Thakur, A. Mahajan, G. Sharma, B. Singh, K. Raza, S. Chhibber and O. P. Katore, *Int. J. Pharm.*, 2020, **576**, 19.
- 145 M. C. G. Pella, M. K. Lima-Tenorio, E. T. T. Neto, M. R. Guilherme, E. C. Muniz and A. F. Rubira, *Carbohydr. Polym.*, 2018, **196**, 233–245.
- 146 V. Dodane and V. D. Vilivalam, *Pharm. Sci. Technol. Today*, 1998, **1**, 246–253.
- 147 C. Velasquillo, P. Silva-Bermudez, N. Vazquez, A. Martinez, A. Espadin, J. Garcia-Lopez, A. Medina-Vega, H. Lecona, R. Pichardo-Baena, C. Ibarra and K. Shirai, *J. Biomed. Mater. Res., Part A*, 2017, **105**, 2875–2891.
- 148 A. P. Deng, Y. Yang, S. M. Du, X. X. Yang, S. C. Pang, X. J. Wang and S. L. Yang, *Mater. Sci. Eng., C*, 2021, **119**, 13.
- 149 J. A. S. Moreno, A. C. Mendes, K. Stephansen, C. Engwer, F. M. Goycoolea, A. Boisen, L. H. Nielsen and I. S. Chronakis, *Carbohydr. Polym.*, 2018, **190**, 240–247.
- 150 S. Rashki, K. Asgarpour, H. Tarrahimofrad, M. Hashemipour, M. S. Ebrahimi, H. Fathizadeh, A. Khorshidi, H. Khan, Z. Marzhooseyni, M. Salavati-Niasari and H. Mirzaei, *Carbohydr. Polym.*, 2021, **251**, 12.
- 151 Z. A. Ahovan, S. Khosravimelal, B. S. Eftekhari, S. Mehrabi, A. Hashemi, S. Eftekhari, P. B. Milan, M. Mobaraki, A. M. Seifalian and M. Gholipourmalekabadi, *Int. J. Biol. Macromol.*, 2020, **164**, 4475–4486.
- 152 G. Kravanja, M. Primožic, Z. Knez and M. Leitgeb, *Molecules*, 2019, **24**, 23.
- 153 F. L. Yan, Q. F. Dang, C. S. Liu, J. Q. Yan, T. Wang, B. Fan, D. S. Cha, X. L. Li, S. G. Liang and Z. Z. Zhang, *Carbohydr. Polym.*, 2016, **149**, 102–111.
- 154 X. F. Liu, Y. L. Guan, D. Z. Yang, Z. Li and K. De Yao, *J. Appl. Polym. Sci.*, 2001, **79**, 1324–1335.
- 155 J. H. Li, Y. G. Wu and L. Q. Zhao, *Carbohydr. Polym.*, 2016, **148**, 200–205.
- 156 S.-H. Eom, S.-K. Kang, D.-S. Lee, J.-I. Myeong, J. Lee, H.-W. Kim, K.-H. Kim, J.-Y. Je, W.-K. Jung and Y.-M. Kim, *J. Microbiol. Biotechnol.*, 2016, **26**, 784–789.
- 157 X. H. Wang, Y. M. Du, L. H. Fan, H. Liu and Y. Hu, *Polym. Bull.*, 2005, **55**, 105–113.
- 158 T. Chhibber, V. S. Gondil and V. R. Sinha, *AAPS PharmSci-Tech*, 2020, **21**, 12.
- 159 E. Luna-Hernandez, M. E. Cruz-Soto, F. Padilla-Vaca, R. A. Mauricio-Sanchez, D. Ramirez-Wong, R. Munoz, L. Granados-Lopez, L. R. Ovalle-Flores, J. L. Menchaca-Arredondo, A. Hernandez-Rangel, E. Prokhorov, J. L. Garcia-Rivas, B. L. Espana-Sanchez and G. Luna-Barcenas, *Int. J. Biol. Macromol.*, 2017, **105**, 1241–1249.
- 160 S. Abid, T. Hussain, A. Nazir, A. Zahir, S. Ramakrishna, M. Hameed and N. Khenoussi, *Int. J. Biol. Macromol.*, 2019, **135**, 1222–1236.
- 161 Y. Chen, H. Y. Qiu, M. H. Dong, B. Cheng, Y. G. Jin, Z. R. Tong, P. W. Li, S. D. Li and Z. M. Yang, *Carbohydr. Polym.*, 2019, **206**, 435–445.
- 162 K. Bankoti, A. P. Rameshbabu, S. Datta, P. Goswami, M. Roy, D. Das, S. K. Ghosh, A. K. Das, A. Mitra, S. Pal, D. Maulik, B. Su, P. Ghosh, B. Basu and S. Dhara, *Biomacromolecules*, 2021, **22**, 514–533.
- 163 J. H. Diaz and F. A. Lopez, *Am. J. Med. Sci.*, 2015, **349**, 269–275.
- 164 J. Dorazilova, J. Muchova, K. Smerkova, S. Kociova, P. Divis, P. Kopel, R. Vesely, V. Pavlinakova, V. Adam and L. Vojtova, *Nanomaterials*, 2020, **10**, 21.
- 165 Q. Q. Ouyang, Z. Hu, Z. P. Lin, W. Y. Quan, Y. F. Deng, S. D. Li, P. W. Li and Y. Chen, *Int. J. Biol. Macromol.*, 2018, **112**, 1191–1198.
- 166 I. Bano, M. Arshad, T. Yasin and M. A. Ghauri, *Int. J. Biol. Macromol.*, 2019, **124**, 155–162.
- 167 J. S. Lu, W. Y. Zhu, L. Dai, C. L. Si and Y. H. Ni, *Carbohydr. Polym.*, 2019, **215**, 289–295.
- 168 G. H. Yan, B. L. Chen, X. H. Zeng, Y. Sun, X. Tang and L. Lin, *Carbohydr. Polym.*, 2020, **244**, 15.
- 169 Z. Wei, J. H. Yang, J. X. Zhou, F. Xu, M. Zrinyi, P. H. Dussault, Y. Osada and Y. M. Chen, *Chem. Soc. Rev.*, 2014, **43**, 8114–8131.
- 170 S. Obuobi, Z. X. Voo, M. W. Low, B. Czarny, V. Selvarajan, N. L. Ibrahim, Y. Y. Yang and P. L. R. Ee, *Adv. Healthcare Mater.*, 2018, **7**, 8.



- 171 Y. Yao, X. D. Chi, Y. J. Zhou and F. H. Huang, *Chem. Sci.*, 2014, **5**, 2778–2782.
- 172 C. Pitzler, G. Wirtz, L. Vojcic, S. Hiltl, A. Boker, R. Martinez and U. Schwaneberg, *Chem. Biol.*, 2014, **21**, 1733–1742.
- 173 J. G. Hardy, M. N. Amend, S. Geissler, V. M. Lynch and C. E. Schmidt, *J. Mater. Chem. B*, 2015, **3**, 5005–5009.
- 174 J. Qu, X. Zhao, Y. P. Liang, Y. M. Xu, P. X. Ma and B. L. Guo, *Chem. Eng. J.*, 2019, **362**, 548–560.
- 175 X. Zhao, R. N. Dong, B. L. Guo and P. X. Ma, *ACS Appl. Mater. Interfaces*, 2017, **9**, 29595–29611.
- 176 X. Xue, Y. Hu, Y. H. Deng and J. C. Su, *Adv. Funct. Mater.*, 2021, **31**, 20.
- 177 B. L. Guo, J. Qu, X. Zhao and M. Y. Zhang, *Acta Biomater.*, 2019, **84**, 180–193.
- 178 I. S. Foulds and A. T. Barker, *Br. J. Dermatol.*, 1983, **109**, 515–522.
- 179 L. C. Kloth and J. M. McCulloch, *Adv. Wound Care*, 1996, **9**, 42–45.
- 180 Y. P. Liang, X. Zhao, T. L. Hu, Y. Han and B. L. Guo, *J. Colloid Interface Sci.*, 2019, **556**, 514–528.
- 181 I. Jun, S. Jeong and H. Shin, *Biomaterials*, 2009, **30**, 2038–2047.
- 182 H. T. Cui, J. Shao, Y. Wang, P. B. Zhang, X. S. Chen and Y. Wei, *Biomacromolecules*, 2013, **14**, 1904–1912.
- 183 N. C. Spitzer, *Nature*, 2006, **444**, 707–712.
- 184 S. H. Ku, S. H. Lee and C. B. Park, *Biomaterials*, 2012, **33**, 6098–6104.
- 185 B. L. Guo, L. Glavas and A. C. Albertsson, *Prog. Polym. Sci.*, 2013, **38**, 1263–1286.
- 186 B. Guo, A. Finne-Wistrand and A.-C. Albertsson, *Macromolecules*, 2012, **45**, 652–659.
- 187 B. Guo, A. Finne-Wistrand and A. C. Albertsson, *Chem. Mater.*, 2011, **23**, 4045–4055.
- 188 L. C. Li, M. Yu, P. X. Ma and B. L. Guo, *J. Mater. Chem. B*, 2016, **4**, 471–481.
- 189 Y. B. Wu, L. Wang, B. L. Guo, Y. P. Shao and P. X. Ma, *Biomaterials*, 2016, **87**, 18–31.
- 190 M. H. Xie, L. Wang, B. L. Guo, Z. Wang, Y. E. Chen and P. X. Ma, *Biomaterials*, 2015, **71**, 158–167.
- 191 Z. X. Deng, Y. Guo, X. Zhao, L. C. Li, R. N. Dong, B. L. Guo and P. X. Ma, *Acta Biomater.*, 2016, **46**, 234–244.
- 192 M. Talikowska, X. X. Fu and G. Lisak, *Biosens. Bioelectron.*, 2019, **135**, 50–63.
- 193 M. Gizdavic-Nikolaidis, J. Travas-Sejdic, G. A. Bowmaker, R. P. Cooney and P. A. Kilmartin, *Synth. Met.*, 2004, **140**, 225–232.
- 194 N. Baheiraei, H. Yeganeh, J. Ai, R. Gharibi, M. Azami and F. Faghihi, *Mater. Sci. Eng., C*, 2014, **44**, 24–37.
- 195 J. Qu, X. Zhao, P. X. Ma and B. L. Guo, *Acta Biomater.*, 2018, **72**, 55–69.
- 196 Z. Kucekova, V. Kasparkova, P. Humpolicek, P. Sevcikova and J. Stejskal, *Chem. Pap.*, 2013, **67**, 1103–1108.
- 197 R. N. Dong, X. Zhao, B. L. Guo and P. X. Ma, *ACS Appl. Mater. Interfaces*, 2016, **8**, 17138–17150.
- 198 Y. P. Liang, B. J. Chen, M. Li, J. H. He, Z. H. Yin and B. L. Guo, *Biomacromolecules*, 2020, **21**, 1841–1852.
- 199 X. M. Dai, Y. Zhao, Y. J. Yu, X. L. Chen, X. S. Wei, X. G. Zhang and C. X. Li, *ACS Appl. Mater. Interfaces*, 2017, **9**, 30470–30479.
- 200 S. J. Park, E. B. Kang, S. M. Sharker, G. Lee, I. In and S. Y. Park, *Macromol. Mater. Eng.*, 2016, **301**, 141–148.
- 201 Y. L. Yu, P. F. Li, C. L. Zhu, N. Ning, S. Y. Zhang and G. J. Vancso, *Adv. Funct. Mater.*, 2019, **29**, 11.
- 202 N. W. S. Kam, M. O'Connell, J. A. Wisdom and H. J. Dai, *Proc. Natl. Acad. Sci. U. S. A.*, 2005, **102**, 11600–11605.
- 203 Z. X. Deng, Y. Guo, X. Zhao, P. X. Ma and B. L. Guo, *Chem. Mater.*, 2018, **30**, 1729–1742.
- 204 J. H. He, M. T. Shi, Y. P. Liang and B. L. Guo, *Chem. Eng. J.*, 2020, **394**, 17.
- 205 L. L. Ma, Y. L. Zhou, Z. W. B. Zhang, Y. Q. Liu, D. Zhai, H. Zhuang, Q. Li, J. D. Yuye, C. T. Wu and J. Chang, *Sci. Adv.*, 2020, **6**, 11.
- 206 B. J. Mai, M. Q. Jia, S. P. Liu, Z. H. Sheng, M. Li, Y. R. Gao, X. B. Wang, Q. H. Liu and P. Wang, *ACS Appl. Mater. Interfaces*, 2020, **12**, 10156–10169.
- 207 M. H. Zheng, X. C. Wang, O. Yue, M. D. Hou, H. J. Zhang, S. Beyer, A. M. Blocki, Q. Wang, G. D. Gong, X. H. Liu and J. L. Guo, *Biomaterials*, 2021, **276**, 10.
- 208 K. Han, Q. Bai, Q. Y. Zeng, N. Sun, C. Y. Zheng, W. D. Wu, Y. N. Zhang and T. L. Lu, *Mater. Des.*, 2022, **217**, 13.
- 209 K. Han, Q. Bai, W. D. Wu, N. Sun, N. Cui and T. L. Lu, *Int. J. Biol. Macromol.*, 2021, **183**, 2142–2151.
- 210 Y. Wang, J. Beekman, J. Hew, S. Jackson, A. C. Issler-Fisher, R. Parungao, S. S. Lajevardi, Z. Li and P. K. M. Maitz, *Adv. Drug Delivery Rev.*, 2018, **123**, 3–17.
- 211 J. A. Burdick and G. D. Prestwich, *Adv. Mater.*, 2011, **23**, H41–H56.
- 212 J. H. Park, E. J. Park and H. S. Yi, *Int. J. Lower Extremity Wounds*, 2017, **16**, 202–207.
- 213 J. A. del Olmo, J. M. Alonso, V. S. Martinez, L. Ruiz-Rubio, R. P. Gonzalez, J. L. Vilas-Vilela and L. Perez-Alvarez, *Mater. Sci. Eng., C*, 2021, **125**, 18.
- 214 H. N. Suo, M. Hussain, H. Wang, N. Y. Zhou, J. Tao, H. Jiang and J. T. Zhu, *Biomacromolecules*, 2021, **22**, 3049–3059.
- 215 Q. B. Dong, X. P. Zhong, Y. Q. Zhang, B. K. Bao, L. Liu, H. H. Bao, C. Y. Bao, X. S. Cheng, L. Y. Zhu and Q. N. Lin, *Carbohydr. Polym.*, 2020, **245**, 9.
- 216 Y. P. Liang, X. Zhao, T. L. Hu, B. J. Chen, Z. H. Yin, P. X. Ma and B. L. Guo, *Small*, 2019, **15**, 17.
- 217 A. Oryan, E. Alemzadeh, J. Tashkhourian and S. F. N. Ana, *Carbohydr. Polym.*, 2018, **200**, 82–92.
- 218 B. D. Zheng, J. Ye, Y. C. Yang, Y. Y. Huang and M. T. Xiao, *Carbohydr. Polym.*, 2022, **275**, 15.
- 219 B. ter Horst, G. Chouhan, N. S. Moiemien and L. M. Grover, *Adv. Drug Delivery Rev.*, 2018, **123**, 18–32.
- 220 Y. Yuan, S. H. Shen and D. D. Fan, *Biomaterials*, 2021, **276**, 17.

